

TrIM: Transformed Iterative Mondrian Forests for Gradient-based Dimension Reduction and High-Dimensional Regression

Ricardo Baptista¹, Eliza O'Reilly², and Yangxinyu Xie³

¹*Computing and Mathematical Sciences Department
California Institute of Technology
rsb@caltech.edu*

²*Department of Applied Mathematics and Statistics
Johns Hopkins University
eoreill2@jh.edu*

³*Department of Statistics and Data Science
University of Pennsylvania
xinyux@wharton.upenn.edu*

Abstract: We propose a computationally efficient algorithm for gradient-based linear dimension reduction and high-dimensional regression. The algorithm initially computes a Mondrian forest and uses this estimator to identify a relevant feature subspace of the inputs from an estimate of the expected gradient outer product (EGOP) of the regression function. In addition, we introduce an iterative approach known as Transformed Iterative Mondrian (TrIM) forest to improve the Mondrian forest estimator by using the EGOP estimate to update the set of features and weights used by the Mondrian partitioning mechanism. We obtain consistency guarantees and convergence rates for the estimation of the EGOP matrix and the random forest estimator obtained from one iteration of the TrIM algorithm. Lastly, we demonstrate the effectiveness of our proposed algorithm for learning the relevant feature subspace across a variety of settings with both simulated and real data.

Keywords and phrases: Dimension reduction, active subspace, relevant feature subspace, Mondrian forest estimator, iterative algorithm.

1. Introduction

Building accurate models and extracting information from data with a very large number of covariates is a difficult challenge in many scientific and engineering applications. Successful machine learning approaches crucially rely on the presence of low-dimensional structure in real-world datasets. Supervised dimension reduction techniques play an important role in addressing the challenges of high-dimensional learning problems. These techniques offer two key benefits: (1) they enhance the explainability of models by identifying a low-dimensional set of features that are most relevant for predicting the response variable; (2) they improve the accuracy and computational efficiency of models in downstream regression and classification tasks by initially mapping the covariates to this low-dimensional relevant feature space. The improved accuracy is particularly important for prediction in high-dimensional settings with limited data.

Many approaches for dimension reduction select a subset of relevant features for prediction from the given set of covariates. These methods, often referred to as feature or variable selection, are generally applied after an initial model has been generated. The selection process involves computing ad-hoc feature importance scores that quantify the influence of each variable on the model output. These scores are then used to determine which variables are most crucial for the model's performance. *Random forests* (Breiman, 2001) are a widely used class of prediction algorithms

that have demonstrated state-of-the-art empirical performance (Fernández-Delgado et al., 2014) and are equipped with several feature importance scores including the Mean Decrease in Impurity (MDI) and Mean Decrease in Accuracy (MDA) (Breiman, 2001). These scores have increased the popularity of the algorithms in applications where insight into the prediction process is highly valued, but they have well-known biases in favoring features with higher entropy or lower dependence on other features (Strobl et al., 2007, 2008). There has been significant effort to study and address these drawbacks (see recent work by Hooker et al. (2021); Agarwal et al. (2023); Bénard et al. (2022) and the references therein) and several alternative approaches for variable selection using random forests have also been proposed (Lundberg et al., 2020; Coleman et al., 2022; Zhu et al., 2015).

Currently, all of the tree-based feature importance measures are limited to evaluating the relevance of a single covariate at a time for predicting the output. The corresponding theoretical results showing that such dimension reduction techniques allow the model to overcome the curse of dimensionality rely on the assumption that the regression model is *sparse*, that is, the output only varies along a small subset of the input dimensions. Instead, a more flexible dimension reduction model assumes that the model output may depend on *all* input coordinates, but only varies along the span of a general low-dimensional subspace of the inputs called the *relevant feature subspace*. This model for dimension reduction is often called a *multi-index model*, or a *ridge function*. In this paper, we study a new approach for dimension reduction and regression that is designed to adapt to the low-dimensional structure captured by this model. The algorithm combines Mondrian random forests with a linear dimension reduction mechanism based on estimating the expected gradient outer product of the function, which captures the relevant feature subspace.

Mondrian random forests (Lakshminarayanan et al., 2014; Balog et al., 2016) are a computationally efficient random forest variant that is generated from a random hierarchical partitioning process called the *Mondrian process* (Roy and Teh, 2008). They were introduced to efficiently handle the online setting where data arrives over time and the estimator is updated accordingly. The partitioning mechanism is also particularly amenable to theoretical analysis. In fact, Mondrian random forests and their generalizations have so far been the only random forest estimators shown to obtain minimax optimal rates of convergence for regression in arbitrary dimension (Mourtada et al., 2020; O’Reilly and Tran, 2024; Cattaneo et al., 2023). The drawback of this algorithm is that the partitioning mechanism is not data-adaptive, and thus the performance suffers in high-dimensional feature spaces as compared to more data-driven random forest algorithms.

In light of these challenges, we propose a new algorithm called *Transformed Iterative Mondrian* (TrIM) forests that incorporates data adaptivity into the Mondrian process through an iterative two-step procedure. First, a set of features made up of linear combinations of the covariates are selected in a data-driven way. Second, a random forest estimator is built using a Mondrian process to hierarchically split the dataset along these selected features. This approach mitigates increased computational costs as the second step retains the efficiency of the Mondrian partitioning method, as well as allowing one to import much of the existing asymptotic theory for Mondrian forests and their generalizations.

More specifically, the first step of our algorithm is to estimate the expected gradient outer product (EGOP) of the regression function. Under the assumption that the regression model is a ridge function, this matrix is a projection onto the relevant feature subspace. We will use an efficient difference quotient approximation as proposed in Trivedi et al. (2014) to estimate this matrix. This approximation requires an initial estimate of the true regression function, which is a standard Mondrian forest estimator in our algorithm. The advantage of using Mondrian forests for this initial estimate is twofold. They are more computationally efficient than kernel estimates when the data set is large (Lakshminarayanan et al., 2016), and they attain minimax optimal risk bounds. Our first theoretical result in Theorem 4 shows consistency and a convergence rate of our EGOP estimator.

The rate depends on properly scaling the parameters of the Mondrian forest, as well as a step size parameter from the difference quotient approximation, with the amount of data.

The second step of our algorithm applies the estimated EGOP to the training inputs and computes a Mondrian forest using this transformed dataset. This step implicitly generates a hierarchical partition of the input space via a *STIT process* (Nagel and Weiss, 2005) that divides the data along a set of features that are linear combinations of the original covariates. The resulting estimator is a particular kind of random tessellation forest (Ge et al., 2019; O’Reilly and Tran, 2022) that we will refer to as an *oblique Mondrian forest*. O’Reilly (2024) recently obtained convergence rates of such estimators illustrating their robustness to error in estimating the projection onto the relevant feature subspace when the underlying regression model is a ridge function. Combining these results with the error estimate of the EGOP gives our second main theoretical result in Theorem 7 that shows consistency and a convergence rate for the estimator obtained from one iteration of the TrIM algorithm.

In this work, we also present simulation and real data experiments that demonstrate the effectiveness of our proposed algorithm. Our results show that TrIM is able to learn the relevant feature subspace and improve the accuracy of the Mondrian forest regression model across a variety of settings. The code to reproduce the numerical results can be found at github.com/Xieyangxinyu/TrIM.

1.1. Related Work

There has been a lot of attention in the statistical literature on learning the relevant feature subspace for a multi-index model. These methods are collectively known as sufficient dimension reduction, and we refer to Cook (2007) and Li (2017) and the references therein for a summary of this literature. We highlight a subset of these linear dimension reduction methods called inverse regression, which broadly aims to estimate the relevant feature subspace by approximating functionals of the covariates conditioned on the response, i.e. $X|Y$. These techniques include Sliced Inverse Regression (SIR) (Li, 1991; Lin et al., 2018) and Sliced Average Variance Estimation (SAVE) (Dennis Cook, 2000). Loyal et al. (2022) used these methods to select linear combinations of covariates as inputs for Breimans’ random forest algorithm and empirically compares the performances. In Section 5 we perform numerical experiments comparing our approach to those from Loyal et al. (2022). A drawback of these inverse regression techniques is that the number of relevant features is not known *a priori*, and so one may miss any relevant features by selecting a set of directions that does not have the ability to span the relevant feature subspace. Another set of approaches use non-parametric methods to approximate gradients of the function and identify the relevant subspace (Xia et al., 2002; Trivedi et al., 2014). We note that most approaches do not account for the subsequent regression step as we do here.

A parallel line of research in the computational modeling literature focuses on high-dimensional function approximation under the linear dimension reduction model of a ridge function. In this literature the relevant feature subspace has been coined the *active subspace* (Constantine et al., 2014). These methods identify the active subspace using the EGOP matrix as in our proposed algorithm. In particular, they extract the subspace components from the dominant eigenvectors of the EGOP matrix. A number of theoretical guarantees have been obtained in this literature for recovery of the active subspace, but the results assume access to gradient evaluations of the function. In particular, Zahm et al. (2020) derived a bound for the approximation error of vector-valued functions based on the eigenvalues of the EGOP matrix. We do not assume access to such gradient measurements in this work. Instead, we perform regression and learn the underlying low-dimensional subspace from paired input-output samples of the function alone. Moreover, we do not require the solution of an eigenvalue problem, which may be costly in high-dimensional settings.

Finally, there have been a few other works that consider an iterative approach of a feature learning or dimension reduction step combined with a subsequent model for prediction. For instance, given a set of importance scores for each feature, one can try to improve the performance of a random forest by only using the features with large importance scores. To avoid removing features that may have some influence even if the importance score is low, one can also use the scores to *reweight* the distribution used to select a set of features along which to make splits in each tree and iterate this procedure by using the reweighted random forest to compute new feature importance scores. This is the mechanism for *iterative random forests* proposed by Basu et al. (2018). We consider a variant of that approach in Section 4.1, where we use a gradient-based feature importance score to reweight the distribution over the covariate dimensions in the Mondrian process. Of course, this approach is limited to updating feature importance scores of the covariates rather than more general features made of linear combinations of covariates. Iterative algorithms that alternatively estimate the EGOP and a regression function kernel machines have been studied as well (Radhakrishnan et al., 2023) where the EGOP and the model are kernel estimators. Neither work has the corresponding statistical guarantees and consistency rates we obtain here for the TrIM algorithm.

1.2. Outline

The remainder of this paper is organized as follows. Section 2 presents the structured regression problem and the general form of the random forest and EGOP estimator we will use to learn the low-dimensional subspace and the regressor. Section 3 introduces our full algorithm built from Mondrian processes and linear transformations of the data called Transformed Iterative Mondrian (TrIM) forests. Section 4 presents the consistency guarantees and Section 5 shows the experimental results on small and large-scale examples.

2. Regression setting and notation

Suppose a data set $\mathcal{D}_n := \{(X_1, Y_1), \dots, (X_n, Y_n)\}$ is given consisting of n i.i.d. samples from a random pair $(X, Y) \in \mathbb{R}^d \times \mathbb{R}$ such that $\mathbb{E}[Y^2] < \infty$. Let μ denote the unknown distribution of X and assume

$$Y = f(X) + \varepsilon, \quad (1)$$

for some unknown function $f : \mathbb{R}^d \rightarrow \mathbb{R}$ and noise ε satisfying $\mathbb{E}[\varepsilon|X] = 0$ and $\text{Var}(\varepsilon|X) = \sigma^2 < \infty$ almost surely. The goal is to estimate the regressor $f(x) = \mathbb{E}[Y|X = x]$, i.e., the conditional mean for the output. We make the additional assumption that the function f has low-dimensional structure as described in the following.

Assumption 1. The function f is of the form

$$f(x) = g(Bx), \quad x \in \mathbb{R}^d, \quad (2)$$

where $g : \mathbb{R}^s \rightarrow \mathbb{R}$ and $B \in \mathbb{R}^{s \times d}$ for $s \leq d$.

This dimension reduction model is commonly referred to as a *multi-index model* or a *ridge function* (Pinkus, 2015; Hastie et al., 2009). This assumption implies that the regression function depends only on the inputs $\langle b_1, x \rangle, \dots, \langle b_s, x \rangle$, where $\{b_i\}_{i=1}^s$ are the rows of B . The subspace $S := \text{span}(\{b_i\}_{i=1}^s)$ will be called the associated *relevant feature subspace* of the model. Our goal in this work is to estimate a function of the form in (2) by simultaneously estimating f and B . Our estimators for f based on random forest models are described in Section 2.1. We will identify B using an EGOP matrix estimate, also known as a diagnostic matrix from the active subspace literature, described in Section 2.2.

2.1. Random forest regression

The approach we will take for estimating f is to build a *random forest estimator* from a random partition of the input space and the data set \mathcal{D}_n . Let \mathcal{P} be a random partition of \mathbb{R}^d . The regression tree estimator based on \mathcal{P} is

$$\hat{f}_n(x, \mathcal{P}) := \sum_{i=1}^n \frac{1_{\{X_i \in Z_x\}}}{\mathcal{N}_n(x)} Y_i, \quad (3)$$

where Z_x is the cell of \mathcal{P} that contains x and $\mathcal{N}_n(x) := \sum_{i=1}^n 1_{\{X_i \in Z_x\}}$ is the number of points in Z_x . If $\mathcal{N}_n(x) = 0$, then it is assumed that $\hat{f}_n(x, \mathcal{P}) = 0$. The random forest estimator based on \mathcal{P} is defined by averaging M i.i.d. copies of the tree estimator, i.e.

$$\hat{f}_{n,M}(x) := \frac{1}{M} \sum_{m=1}^M \hat{f}_n(x, \mathcal{P}_m), \quad (4)$$

where $\mathcal{P}_1, \dots, \mathcal{P}_M$ are M i.i.d. copies of \mathcal{P} . The performance and asymptotic properties of this estimator depends on how the partition \mathcal{P} is generated.

2.2. Estimation of the expected gradient outer product

The first step of our algorithm will be a feature learning step that computes a linear transformation approximating a projection onto the relevant feature subspace S . We use a gradient-based approach as described in the introduction, and begin by defining the *expected gradient outer product* (EGOP) matrix

$$H = \mathbb{E}[\nabla f(X) \nabla f(X)^T]. \quad (5)$$

This matrix $H \in \mathbb{R}^{d \times d}$ corresponds to the second moment of the random variable $\nabla f(X)$. Thus, it accounts for the variance of the gradient of f with respect to the d inputs. Moreover, the projection $v^T H v$ along any input direction $v \in \mathbb{R}^d$ measures the variability of the gradient of f in this direction. If the variability is small along v , then f can be interpreted having a nearly constant gradient along v on average over the support of X .

If we suppose f satisfies (2) for $B \in \mathbb{R}^{s \times d}$, then $\nabla f(x) = B^T \nabla g(Bx)$, and

$$H = B^T \mathbb{E}[\nabla g(BX) \nabla g(BX)^T] B.$$

Thus, the rank of H is at most s , and the image of H is contained in the relevant feature subspace S . This motivates constructing the expected gradient outer product matrix to identify S . Without knowledge of the functional form of f or the distribution of X , however, one must proceed by obtaining an approximation of H . In our algorithm, we will use the approximation proposed in [Trivedi et al. \(2014\)](#) using the second-order difference quotient approximations of the derivatives.

Given the data set \mathcal{D}_n and an initial estimator \hat{f}_n of f , we first consider for each $j \in [d]$ the second-order difference quotient estimator $\Delta_{j,t} \hat{f}_n(x)$ of $\partial_j f(x)$ for a step size $t > 0$. That is, for a function $g : \mathbb{R}^d \rightarrow \mathbb{R}$,

$$\Delta_{j,t} g(x) := \frac{g(x + te_j) - g(x - te_j)}{2t} \quad (6)$$

is the second-order difference quotient approximation to the derivative of g at x . We then define the vector $\widehat{\nabla}_t \widehat{f}_n(x) \in \mathbb{R}^d$ for $x \in \mathbb{R}^d$ which is an approximation of the gradient vector $\nabla f(x)$ given step size t . For each $j = 1, \dots, d$, we define

$$(\widehat{\nabla}_t \widehat{f}_n(x))_j := \Delta_{j,t} \widehat{f}_n(x) \mathbb{1}_{E_{n,t,j}(x)}, \tag{7}$$

where $E_{n,t,j}(x)$ is the event that the cells containing $x + te_j$ and $x - te_j$ also contain training data. Finally, let $\mathcal{X}_n = \{x_i\}_{i=1}^n$ be i.i.d. samples of the input random variable X that are independent of \mathcal{D}_n . The empirical approximation of H is then given by the matrix

$$\widehat{H}_{n,t} := \frac{1}{n} \sum_{i=1}^n \widehat{\nabla}_t \widehat{f}_n(x_i) \widehat{\nabla}_t \widehat{f}_n(x_i)^T. \tag{8}$$

3. TrIM: Transformed Iterative Mondrian Forests

The approach we propose in this paper to estimate the regressor $f(x) = \mathbb{E}[Y|X = x]$ is to combine a feature learning step consisting of a data driven choice of linear transformation of the input data, and the computation of a Mondrian forest estimator. Mondrian forests (Lakshminarayanan et al., 2014, 2016; Balog et al., 2016) belong to a computationally efficient class of random forest estimators, obtained as in (4) where the random partition \mathcal{P} is generated using a *Mondrian process*. This stochastic process is parameterized by a *lifetime* $\lambda > 0$, which determines the complexity of the random partition.

The construction of a Mondrian tree with lifetime λ restricted to an axis-aligned box in \mathbb{R}^d is shown in Algorithm 1. The Mondrian tree generating process is a recursive algorithm that partitions the input data into smaller and smaller blocks, where the partitioning is determined by the Mondrian process. The process is defined by a set of independent exponential clocks, one for each dimension of the input space. The first clock to ring determines the dimension of the split, and the point of the split is chosen uniformly at random from the range of the data along that dimension. The process is terminated when the first clock to ring has a time greater than the lifetime λ . An illustration of a Mondrian tree is shown in Figure 1.

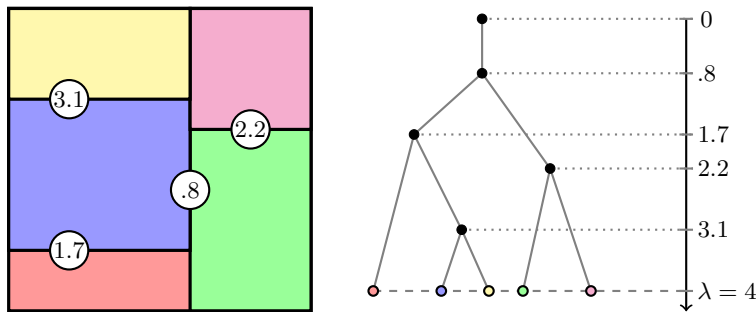


Fig 1: An illustration of the axis-aligned hierarchical partition generated by a Mondrian process with lifetime $\lambda = 4$ and the associated tree embedded on a vertical time axis.

As is clear from the construction, an important hyperparameter for Mondrian forests is the *lifetime* parameter λ , which determines how long the Mondrian partitioning process is run. The choice of this parameter determines the complexity of the estimator and thus it should depend

Algorithm 1: Mondrian Tree Generating Process

Input: A dataset X , lifetime λ , and dimension d
Output: A partition of X into subsets based on the Mondrian partitioning process

- 1 **for** each dimension $c \in [d]$ **do**
- 2 Compute the lower bound l_c and upper bound u_c of X along dimension c
- 3 Associate an independent exponential clock with rate $|u_c - l_c|$ to dimension c
- 4 **end**
- 5 $T \leftarrow$ time of the first clock to ring
- 6 $d \leftarrow$ dimension of the clock that rang first
- 7 **if** $T > \lambda$ **then**
- 8 **return** *Terminate the process*
- 9 **end**
- 10 Choose a point ξ uniformly at random from $[l_c, u_c]$
- 11 Split X into $X_{<} = \{x \in X | x_c < \xi\}$ and $X_{\geq} = \{x \in X | x_c \geq \xi\}$ with a hyperplane perpendicular to X_c at point ξ
- 12 Discard the remaining $d - 1$ clocks
- 13 Recursively call the Mondrian Tree Generating Process with parameter $(X_{<}, \lambda, d)$
- 14 Recursively call the Mondrian Tree Generating Process with parameter (X_{\geq}, λ, d)

on the amount of data available. This has been observed theoretically by Mourtada et al. (2020), O'Reilly and Tran (2024) and O'Reilly (2024), where minimax rates of convergence for Mondrian forests and their generalizations are obtained only with precise tuning of the lifetime parameter with the amount of data points n . The importance of this parameter will be also highlighted in the forthcoming theoretical results and numerical experiments.

The Mondrian process has many appealing computational properties such as the Markov property and spatial consistency, which make Algorithm 1 amenable to efficient online algorithms. The major drawback, as described in the introduction, is that the process is not data-adaptive. This shortcoming becomes particularly problematic in high-dimensional settings where learning from features is essential for achieving good performance. To address this, we propose a novel two-phase approach. First, we apply a data-adaptive linear transformation to the input data; then, we compute a Mondrian forest on the transformed data. We first dive into the details of the first step, which can be interpreted as a generalized form of feature selection: creating a new set of features based on linear combinations of covariates in the original input space. To compute the linear transformation matrix, we first train a Mondrian forest estimator \hat{f}_n on the data set \mathcal{D}_n with lifetime λ using Algorithm 1. We then compute the approximation $\hat{H}_{n,t}$ as in (8) to the expected gradient outer product H by approximating the gradient vector at each point in the data set and taking an average of outer products of the gradient vectors. The pseudocode for computing $\hat{H}_{n,t}$ is shown in Algorithm 2. In Theorem 4 of Section 4, we prove consistency of this estimator for H and obtain a convergence rate for the estimation of ridge functions given a particular scaling of the parameters λ and t with respect to the amount of data n .

Before applying the linear transformation, we normalize the matrix $\hat{H}_{n,t}$ to avoid adjusting the lifetime parameter λ . Specifically, we compute the normalized matrix

$$A_n = d \cdot \hat{H}_{n,t} / \|\hat{H}_{n,t}\|_{2,1}, \quad (9)$$

where the $L_{2,1}$ norm $\|\cdot\|_{2,1}$ is given by the sum of the Euclidean norms of the columns of the matrix, i.e., $\|A\|_{2,1} = \sum_{j=1}^d \|A_{\cdot,j}\|_2$. This normalization ensures that the lifetime parameter λ remains the same for the oblique Mondrian forest estimator $\hat{f}_{n,\lambda}^+$ obtained by training a Mondrian forest $\hat{f}_{n,\lambda}$ on



Fig 2: The original 2-dimensional Euclidean space is transformed by rotating by 10 degrees clockwise and scales the x-axis by 0.9 and y-axis by 0.8. In other words, the original space is transformed by the matrix $A = \begin{bmatrix} 0.8 \cos(10^\circ) & -0.7 \sin(10^\circ) \\ \sin(10^\circ) & 0.8 \cos(10^\circ) \end{bmatrix}$. The Mondrian cuts are made in the transformed space and then transformed back to the original space by applying A^{-1} . Left: The Mondrian cuts in the transformed space. Right: The Mondrian cuts in the original space.

Algorithm 2: Pseudocode for computing $\widehat{H}_{n,t}$

Input: $\mathcal{D}_n = \{(x_i, y_i)\}_{i=1}^n \subset \mathbb{R}^d \times \mathbb{R}$; step size $t > 0$; lifetime $\lambda > 0$; a (transformed) Mondrian forest estimator $\widehat{f}_{n,\lambda}$ on \mathcal{D}_n

Output: Estimated gradient outer product matrix $\widehat{H}_{n,t}$

```

1 for each point  $x \in \mathcal{D}_n$  do
2   for each dimension  $j = 1$  to  $d$  do
3     Compute the approximation of the  $j$ -th component of the gradient vector at  $x$ :

```

$$(\widehat{\nabla} \widehat{f}_{n,\lambda}(x))_j := \frac{\widehat{f}_{n,\lambda}(x + te_j) - \widehat{f}_{n,\lambda}(x - te_j)}{2t}$$

```

4   end
5 end

```

6 Compute the matrix $\widehat{H}_{n,t}$ as an average of outer products of the gradient vectors:

$$\widehat{H}_{n,t} := \frac{1}{n} \sum_{i=1}^n \widehat{\nabla}_t \widehat{f}_{n,\lambda}(x_i) \widehat{\nabla}_t \widehat{f}_{n,\lambda}(x_i)^T$$

the transformed data set $\mathcal{D}_n^+ = \{(A_n x_i, y_i)\}_{i=1}^n$, see Lemma 6. Once we have computed the linear transformation A_n , we transform the data set \mathcal{D}_n by applying A_n to each point. We then compute a Mondrian forest estimator using the transformed data set $\mathcal{D}_n^+ = \{(A_n x_i, y_i)\}_{i=1}^n$ with lifetime λ , which implicitly computes an oblique Mondrian forest estimator $\widehat{f}_{n,\lambda}^+$. Algorithm 3 presents pseudocode describing this procedure. With appropriate scaling of λ and t with respect to the amount of data n , Theorem 7 in Section 4 proves the consistency of this estimator as well as provides

a fast convergence rate as n goes to infinity.

Algorithm 3: Pseudocode for computing estimator $\hat{f}_{n,\lambda}^+$

Input: $\mathcal{D}_n = \{(x_i, y_i)\}_{i=1}^n \subset \mathbb{R}^d \times \mathbb{R}$; lifetime parameter $\lambda > 0$; number of trees M ; transformation matrix $\hat{H}_{n,t}$
Output: Mondrian forest estimator $\hat{f}_{n,\lambda}^+$

1 Compute the normalized matrix

$$A_n = d \cdot \frac{\hat{H}_{n,t}}{\|\hat{H}_{n,t}\|_{2,1}}$$

2 Transform data set \mathcal{D}_n : for each $i = 1, \dots, n$, $x_i \mapsto A_n x_i$; i.e. Set $\mathcal{D}_n^+ = \{(A_n x_i, y_i)\}_{i=1}^n$

3 Compute Mondrian forest estimator $\hat{f}_{n,\lambda}^+$ consisting of M Mondrian trees with lifetime λ on the transformed dataset \mathcal{D}_n^+ using Algorithm 1

4 Return $\hat{f}_{n,\lambda}^+$ where $\hat{f}_{n,\lambda}^+(x) := \hat{f}_{n,\lambda}^+(A_n x)$

We can extend this approach by iteratively updating the linear transformation $\hat{H}_{n,t}$ and the Mondrian forest estimator $\hat{f}_{n,\lambda}^+$ to improve the performance of the estimator until some stopping criterion is met. This leads to our overall algorithm, which we call the *Transformed Iterative Mondrian (TrIM) Forest*. The pseudocode for TrIM is shown in Algorithm 4.

Algorithm 4: Transformed Iterative Mondrian (TrIM) Forest

Input: $\mathcal{D}_n = \{(x_i, y_i)\}_{i=1}^n \subset \mathbb{R}^d \times \mathbb{R}$; lifetime parameter $\lambda > 0$; number of iterations K ; step-size $t > 0$

Output: Mondrian forest estimator $\hat{f}_{n,\lambda}^+$

1 $\hat{H}_{n,t} \leftarrow I_d$

2 **for** $k = 1$ **to** K **do**

3 Given \mathcal{D}_n, λ and $\hat{H}_{n,t}$, compute the transformed Mondrian forest estimator $\hat{f}_{n,\lambda}^+$ using Algorithm 3

4 Compute the linear transformation matrix $\hat{H}_{n,t}^+$ using Algorithm 2 with input $\mathcal{D}_n, t, \lambda, \hat{f}_{n,\lambda}^+$

5 Set $\hat{H}_{n,t} \leftarrow \hat{H}_{n,t}^+$

6 **end**

4. Theoretical Results

In this section, we provide theoretical justification for our algorithm by providing a rate of convergence for the expected error of the estimated EGOP matrix (see Theorem 4) as well as for the subsequent oblique Mondrian estimator (see Theorem 7). To do so, we make the following assumptions about the distribution μ of the input random variable. First recall that a function $f : \mathbb{R}^d \rightarrow \mathbb{R}$ is L -Lipschitz if $\|f(x) - f(y)\|_2 \leq L\|x - y\|_2$ for all $x, y \in \mathbb{R}^d$.

Assumption 2. Assume the distribution μ has compact and convex support K with a density p that is C_p -Lipschitz and strictly positive on its support.

We will also assume the regression function satisfies the following regularity condition.

Assumption 3. Assume $f : W \rightarrow \mathbb{R}$ satisfies, for some finite $L > 0$,

$$\|\nabla f(x) - \nabla f(y)\|_2 \leq L\|x - y\|_2 \text{ and } \|\nabla f(x)\|_2 \leq L, \text{ for all } x, y \in W.$$

Assume the domain W is a compact and convex d -dimensional subset of \mathbb{R}^d .

Our first main result is the following asymptotic error bound on the expected error of the estimator \widehat{H}_n of the EGOP H defined in (8) as the amount of data n grows. Recall the estimator depends on the lifetime parameter λ of the initial Mondrian forest estimator and the stepsize parameter t in the difference quotient approximation. To obtain consistency of this estimator, the lifetime must grow to infinity, and the stepsize decay to zero appropriately with n . Throughout, $\|\cdot\|$ will denote the operator norm of a matrix.

Theorem 4. *Let μ and f satisfy Assumptions 2 and 3. Let $\widehat{H}_n = \widehat{H}_{n,t_n,\lambda_n}$ be the estimator of H as in (8) built from a Mondrian forest estimator \widehat{f}_n with lifetime λ_n and number of trees M_n . Letting $\lambda_n \sim n^{\frac{1}{d+3}}$, $M_n \gtrsim n^{\frac{1}{d+3}}$ and $t_n \sim n^{-\frac{3}{4d+12}}$ as $n \rightarrow \infty$ gives*

$$\mathbb{E}[\|\widehat{H}_n - H\|] \lesssim n^{-\frac{3}{4d+12}},$$

where the expectation is taken with respect to \mathcal{D}_n , \mathcal{P} , and \mathcal{X}_n .

As a corollary we obtain an approximation rate of the normalized matrix A_n defined in (9) that we apply to the data in Algorithm 3.

Corollary 5. *Consider the setting of Theorem 4. Letting $\lambda_n \sim n^{\frac{1}{d+3}}$, $M_n \gtrsim n^{\frac{1}{d+3}}$ and $t_n \sim n^{-\frac{3}{4d+12}}$ as $n \rightarrow \infty$ gives*

$$\mathbb{E}[\|A_n - A\|_{2,1}] \lesssim n^{-\frac{3}{4d+12}},$$

where $A := d \cdot H / \|H\|_{2,1}$, and the expectation is taken with respect to \mathcal{D}_n , \mathcal{P} , and \mathcal{X}_n .

The proofs of the above results appear in Appendix A. The proof of Theorem 4 follows from a risk bound on the estimation of the gradient of f via the second order difference quotient, which relies on the asymptotic behavior of the expected risk for a Mondrian forest estimator with respect to the input shifted by t_n .

We next turn to proving a convergence rate for the estimator of the regressor f obtained from Algorithm 3 after applying the learned transformation A_n to the input data. We first characterize the distribution of the random partition of the original data \mathcal{D}_n induced by this algorithm. Indeed, O'Reilly and Tran (2022) (see also O'Reilly (2024)) showed that the random partition of the data obtained by applying a linear transformation and then running a Mondrian process has the same distribution as randomly partitioning the data with a *stable under iteration (STIT) process* (Nagel and Weiss, 2005) with a discrete directional distribution determined by the linear transformation. The distribution and construction of a STIT process is determined by a *lifetime* parameter $\lambda > 0$ and a probability measure ϕ on \mathbb{S}^{d-1} called the *directional distribution*, which governs the directions where partitioning occurs. When the directional distribution ϕ is uniform over the standard unit basis vectors, the corresponding STIT process with lifetime λ is the same as the Mondrian process with lifetime λ . For more on this general class of random partitioning processes, the corresponding class of oblique random forests, and their applications, we refer the reader to O'Reilly and Tran (2022, 2024) and the references therein. Following O'Reilly (2024), we will refer to STIT forests where ϕ is a discrete measure as *oblique Mondrian forests*. The following result follows immediately from Proposition 17 by O'Reilly (2024).

Lemma 6. *The estimator \widehat{f}_n output by Algorithm 3 is an oblique Mondrian forest estimator with M trees, lifetime λ and directional distribution*

$$\phi_n = \sum_{i=1}^d \frac{\|a_i^{(n)}\|_2}{\|A_n\|_{2,1}} \delta_{a_i^{(n)}/\|a_i^{(n)}\|_2},$$

where $(a_1^{(n)}, \dots, a_d^{(n)})$ are the columns of $A_n \in \mathbb{R}^{d \times d}$ and $\|\cdot\|_{2,1}$ is the $L_{2,1}$ norm. The $L_{2,1}$ norm is the sum of the Euclidean norms of the columns of the matrix, i.e.

$$\|A_n\|_{2,1} := \sum_{i=1}^d \|a_i^{(n)}\|_2.$$

Recall that from Algorithm 3, $\|A_n\|_{2,1} = d$.

We now obtain an upper bound on the expected risk of an honest version of the estimator obtained from Algorithm 3 when the underlying regression function f is assumed to be a ridge function. The honest version of the estimator assumes the matrix A_n is applied to a dataset \mathcal{D}'_n independent of the original dataset \mathcal{D}_n used to compute A_n and the forest is built from a collection \mathcal{P}' of Mondrian processes independent from those used to obtain A_n . The proof can be found in Appendix B.

Theorem 7. *Assume μ satisfies Assumption 2 and f satisfies (2) for a function $g: \mathbb{R}^s \rightarrow \mathbb{R}$ satisfying Assumption 3. For each n , let \hat{f}_n be the oblique Mondrian forest obtained from Algorithm 3 with lifetime parameter $\lambda_n > 0$, number of trees M_n , and transformation matrix \hat{H}_n as in Theorem 4 that is independent of \hat{f}_n . Assume $\lambda_n \sim n^{\frac{1}{d+2} + \frac{3(1-\delta)(d-s)}{4(d+3)(d+2)}}$ and $M_n \gtrsim \lambda_n$. For $\delta \in [0, 1)$, for all n large enough, we have that with probability greater than $1 - Cn^{-\frac{3\delta}{4d+12}}$,*

$$\mathbb{E}[(\hat{f}_n(X) - f(X))^2] \lesssim n^{-\frac{2}{d+2} - \frac{3(1-\delta)(d-s)}{2(d+3)(d+2)}}.$$

Remark 8. The result of Theorem 7 provides a convergence rate for a TrIM forest after one iteration under the assumption the regression function f is a ridge function. For $s = d$, this rate matches that obtained for Mondrian and STIT random forests for Lipschitz functions f (Mourtada et al., 2020; O'Reilly and Tran, 2024), and improves on this rate for $s < d$. While it is challenging to account for dependencies between estimators for f and A in the repeated iterations, we expect the dependence on d to become milder as the estimate of A improves. Indeed, with the correct knowledge of the low-dimensional subspace, the convergence rate should scale as $n^{-2/(s+2)}$. In effect, this corresponds to the case $d = s$.

4.1. Weighted Mondrian estimators

We now consider the setting where the algorithm is restricted to reweighting the axis-aligned cuts of a Mondrian process and we assume that the regression function is *sparse*. That is, let $S \subseteq \{1, \dots, d\}$ be a subset of size $|S| = s$ that corresponds to a low dimensional set of relevant feature dimensions. Assume the regression setting of Section 2 and additionally that the true function f is of the form

$$f(x) = g(x_S) = g(\{x_i\}_{i \in S}), \quad (10)$$

for some function $g: \mathbb{R}^s \rightarrow \mathbb{R}$. This study is motivated by the models considered in the iterative random forests algorithm Basu et al. (2018) and Deng et al. (2022), which computes single-covariate feature scores to identify S .

For a Mondrian forest estimator \hat{f}_n of f built from the training data \mathcal{D}_n and each covariate index i , we can define the feature importance score

$$\omega_i^{(n,t)} = \frac{1}{n} \sum_{j=1}^n |(\hat{\nabla}_t \hat{f}_n(x_j))_i|^2, \quad (11)$$

where $\widehat{\nabla}_t \widehat{f}_n(x)$ is the gradient estimator as defined in (7) and $\mathcal{X}_n = \{x_j\}_{j=1}^n$ are n i.i.d. samples of the input random variable X that are independent of \mathcal{D}_n . Note that these scores form the diagonal of the EGOP estimator (8).

In Theorem 9 below we first show that these weights, with appropriate tuning of the parameters with n , are consistent estimators of the diagonal of the EGOP matrix normalized to have unit trace, which are nonzero for relevant covariate indices $i \in S$ and zero for $i \notin S$.

Theorem 9. *Let \widehat{f}_n be a Mondrian forest estimator with lifetime $\lambda_n > 0$ and number of trees M_n of a function f as in (10) for some set of relevant features S and g satisfying Assumption 3. For each $i \in [d]$, let $\omega_i^{(n)} := \omega_i^{(n, t_n)}$ be defined as in (11). Then, letting $\lambda_n \sim n^{\frac{1}{d+3}}$, $M_n \gtrsim n^{\frac{1}{d+3}}$ and $t_n \sim n^{-\frac{3}{4d+12}}$ as $n \rightarrow \infty$ gives*

$$\mathbb{E} \left[\max_{i \in \{1, \dots, d\}} \left| \frac{\omega_i^{(n)}}{\sum_{j=1}^d \omega_j^{(n)}} - \frac{\mathbb{E}[|(\nabla f(X))_i|^2]}{\mathbb{E}[\|\nabla f(X)\|_2^2]} \right| \right] \lesssim n^{-\frac{3}{4d+12}}.$$

where the expectation is taken with respect to \mathcal{X}_n , \mathcal{P} and \mathcal{D}_n .

Now consider an updated *weighted* Mondrian forest estimator built from n i.i.d. samples of (X, Y) that are independent of \mathcal{D}_n , and M_n Mondrian trees with lifetime $\lambda_n > 0$ and directional distribution

$$\phi_n = \sum_{i=1}^d \frac{\omega_i^{(n)}}{\sum_{j=1}^d \omega_j^{(n)}} \delta_{e_i}, \quad (12)$$

where the weights $\omega_i^{(n)} > 0$ determining how often covariates are split in the partitioning process are obtained from the feature importance scores defined in (11). Theorem 10 gives an asymptotic upper bound on the expected quadratic risk of this weighted Mondrian forest estimator. The proofs of these results are found in Appendix 10.

Theorem 10. *Assume $\text{supp}(\mu) = [0, 1]^d$ and that μ has a positive and Lipschitz density on its support. Let \widehat{f}_n be the weighted Mondrian forest estimator with directional distribution (12), lifetime $\lambda_n > 0$, and number of trees M_n of a function f as in (10) for some set of relevant features S and g satisfying Assumption 3. Let $M_n \gtrsim \lambda_n$ and $\lambda_n \sim n^{\frac{1}{d+3} + \frac{3(d-s)}{4(d+3)^2}}$. Then for all n large enough, with probability at least $1 - Cn^{-\frac{3\delta}{4d+12}}$ with respect to \mathcal{D}_n , \mathcal{P} , and \mathcal{X}_n ,*

$$\mathbb{E}[(\widehat{f}_n(X) - f(X))^2] \lesssim n^{-\frac{3}{d+3} - \frac{9(d-s)}{4(d+3)^2}}.$$

Remark 11. If the quadratic risk is conditioned on the input being a fixed distance from the boundary of the support, i.e. $X \in [\delta, 1 - \delta]^d$ for some $\delta \in (0, 1/2)$, one obtains for $s < d$ a rate of convergence above that is faster than the minimax optimal rate of convergence $n^{-4/d+4}$ for general functions on \mathbb{R}^d satisfying Assumption 3.

5. Simulation Studies

Our simulation experiments aim to demonstrate how the proposed TrIM method from Section 3 can identify the relevant feature subspace and leverage this structure for prediction. We consider four different ridge functions of the form $f(x) = g(Bx)$ for some low-rank matrix $B \in \mathbb{R}^{s \times d}$ and $g: \mathbb{R}^s \rightarrow \mathbb{R}$ with $d = 5$ and $s = 2$. In particular, we consider the combinations of two transformation matrices B and two functions g . To define the relevant subspace, we consider the following two transformations:

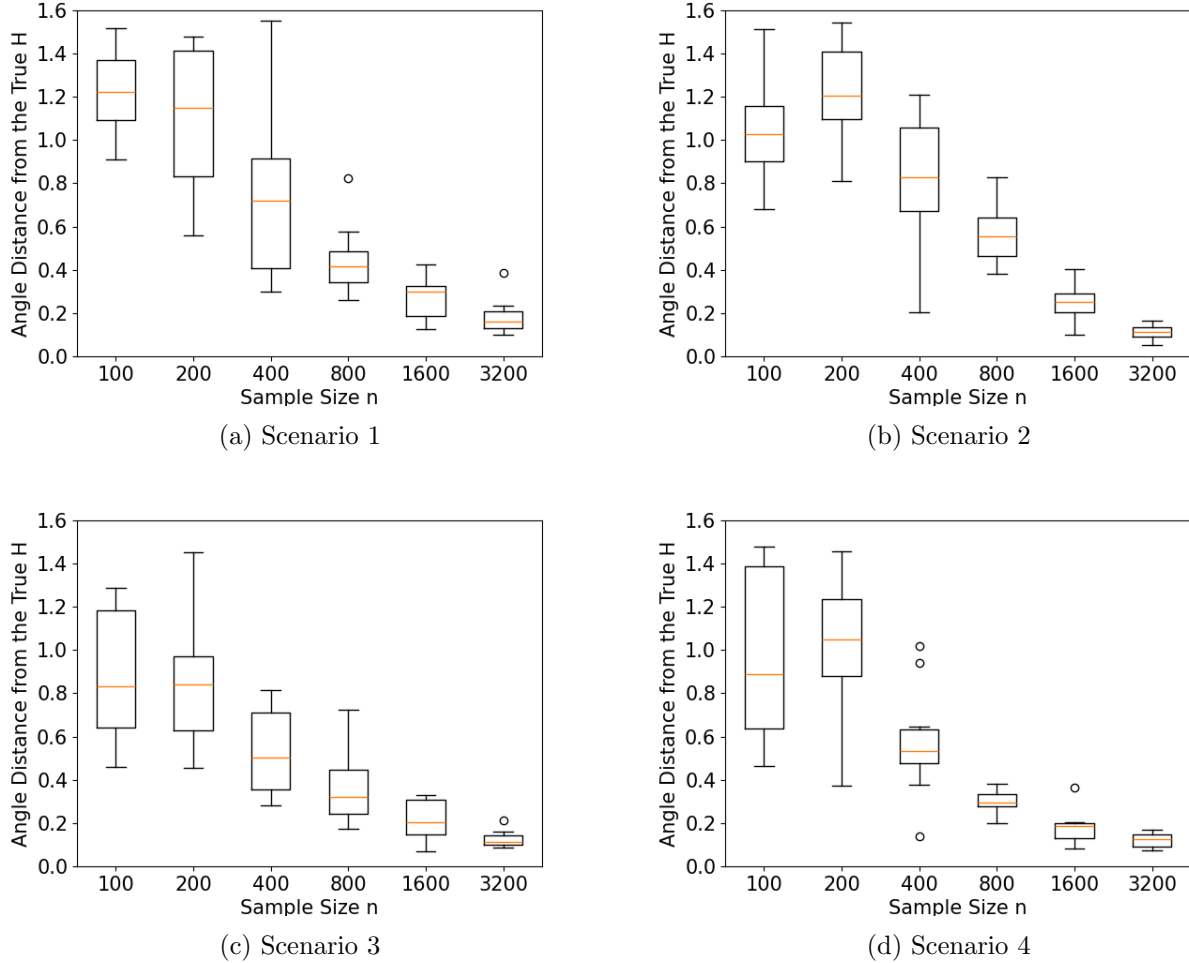


Fig 3: Maximum principal angles between the subspaces spanned by the expected outer product matrix H and estimated expected outer product matrix $\hat{H}_{n,t}$ for different scenarios. This confirms the theoretical results that the estimated expected outer product matrix $\hat{H}_{n,t}$ converges to the true expected outer product matrix H as the training sample size increases.

1. The first row of B_1 captures dependence on the first three inputs, and the second row of B_1 captures the dependence of all but the third input.

$$B_1 = \begin{bmatrix} 1 & 1 & 1 & 0 & 0 \\ 1 & 1 & 0 & 1 & 1 \end{bmatrix}.$$

2. B_2 contains the first two rows of a random matrix from the orthogonal group $O(5)$. Specifically, we consider

$$B_2 = \begin{bmatrix} -0.49424072 & 0.11211344 & -0.27421644 & -0.62783889 & 0.52324025 \\ -0.0014017 & 0.71072528 & 0.69059226 & -0.11064719 & 0.07554563 \end{bmatrix}.$$

For the predictive task, we consider the two regression functions: $g_1(x) = x_1^4 + x_2^4$ and $g_2(x) = \exp(-0.25 \min(x_1^2, x_2^2))$. This leads to four different scenarios: (1) $f(x) = g_1(B_1x)$, (2) $f(x) = g_2(B_1x)$, (3) $f(x) = g_1(B_2x)$ and (4) $f(x) = g_2(B_2x)$.

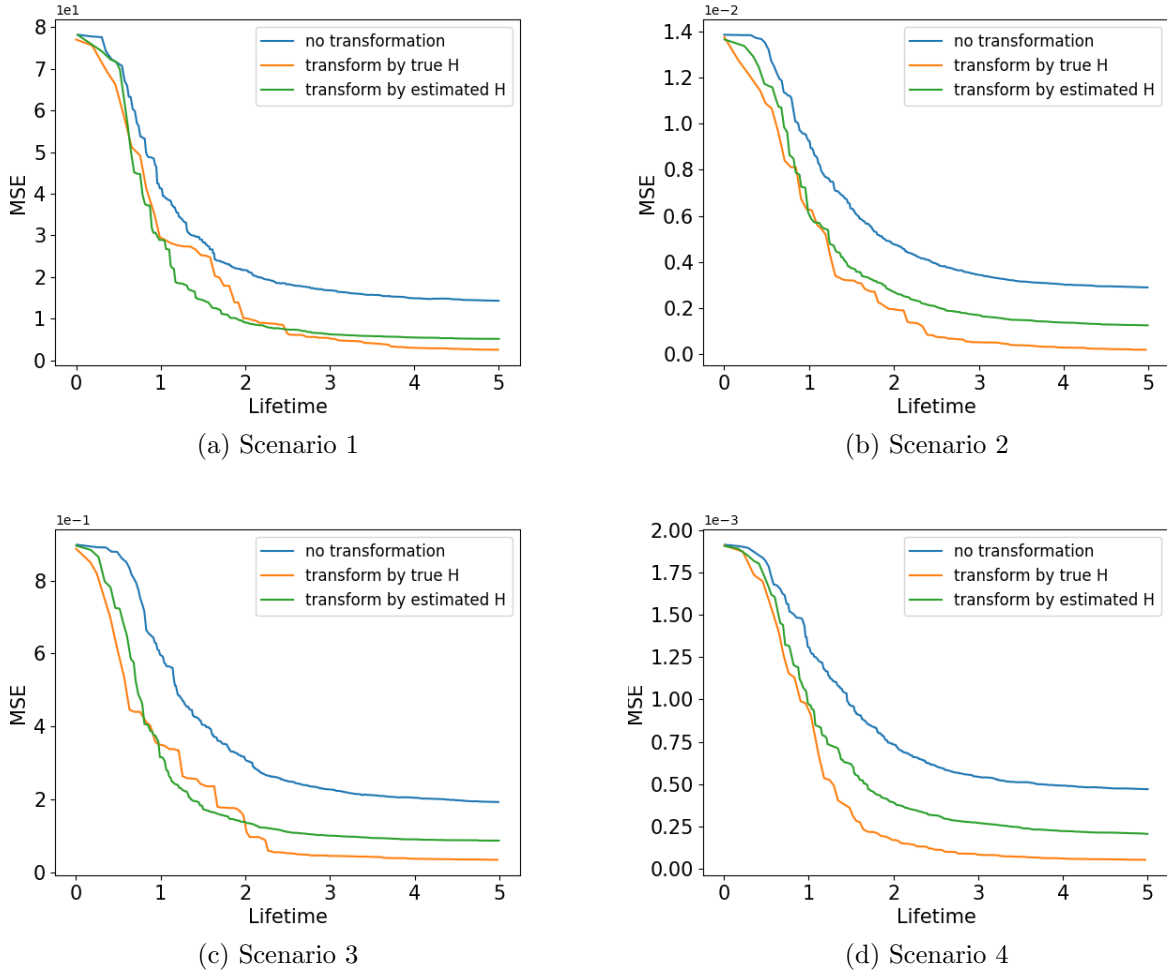


Fig 4: Comparison of the test mean squared error (MSE) of three different methods: Baseline, Proposed, and Oracle.

For each scenario, we set the maximum lifetime parameter $\lambda = 5$, the number of Mondrian trees $B = 10$, the step size $t = 0.1$, the inputs $X \sim U[0, 1]^d$, and noise $\varepsilon \sim \mathcal{N}(0, \sigma^2 = 0.01)$. We set the training sample size to at most 3200 and the test sample size to 1000.

For the first experiment, we vary the training sample size $n \in \{100, 200, 400, 800, 1600, 3200\}$ and evaluate the recovery of the low-dimensional relevant feature subspace using the TrIM method. In particular, we compare the maximum principle angles between the subspaces spanned by the EGOP matrix H and estimated EGOP matrix $\hat{H}_{n,t}$. The value of the principle angles range from 0 to $\pi/2$ (Ye and Lim, 2016). We refer the reader to Appendix D for the definition and interpretation of the maximum principal angle. The true EGOP matrix in (5) is estimated based on exact evaluations of the gradient ∇f , which are computed using the Python package JAX (Bradbury et al., 2018) at the test samples. The estimated EGOP matrix is calculated by our proposed method using the training samples, as described in Algorithm 2.

As shown in Figure 3, across all scenarios, the maximum principal angles between the subspaces spanned by the EGOP matrix H and estimate $\hat{H}_{n,t}$ decrease as the training sample size increases. This aligns with the theoretical result that $\hat{H}_{n,t}$ converges to the true EGOP matrix H as the

training sample size increases; see Theorem 4.

For the second experiment, we use the estimated EGOP matrix $\widehat{H}_{n,t}$ to transform the data and construct the Mondrian forest estimator with lifetime λ from 0 to 5 using Algorithm 3. For each scenario, we set the training sample size to $n = 3200$ and compare the test mean squared error (MSE) of three different methods:

- **Baseline:** Mondrian forest estimator with lifetime λ without transforming the data;
- **Proposed:** Mondrian forest estimator with lifetime λ after transforming the data using the estimated EGOP matrix $\widehat{H}_{n,t}$;
- **Oracle:** Mondrian forest estimator with lifetime λ after transforming the data using the EGOP matrix H .

Figure 4 shows that the test MSE of the proposed method is consistently lower than the baseline across all scenarios. This suggests that the proposed method can effectively identify the relevant feature subspace and leverage this knowledge for predictive tasks. Moreover, there is only a small gap between the test MSE of the proposed and oracle method.

In the next two experiments, we show that it is possible to decrease the gap with the oracle method by iterating the proposed method, i.e., we run Algorithm 4 with $K = 2$ by using the updated Mondrian forest to estimate a second outer gradient product matrix. As the figures are similar to the previous experiment, we present them in Appendix E.1. As shown in Figure 6, after one round of the iteration, the principal angles between the subspaces spanned by the EGOP matrix H and the updated version of the estimate $\widehat{H}_{n,t}$ are smaller than the principal angles between the subspaces spanned by H and the original estimate $\widehat{H}_{n,t}$ shown in Figure 3. This suggests that multiple iterations of the proposed method can improve the estimation of H and further decrease the test MSE. In fact, as shown in Figure 7, the test MSE after the second iteration of the proposed method is closer to the test MSE of the oracle method than the test MSE of the proposed method with a single iteration. Future work will establish rigorous convergence rates for multiple iterations of the TrIM forest estimator.

6. Real Data Applications

In this section, we apply our proposed method to two real data applications: a model for the spread of Ebola in Western Africa considered in Constantine and Howard (2016), and multiple predictive machine learning tasks from the UCI Machine Learning Repository (Dua and Graff, 2019).

First, we consider a modified SEIR model for the spread of Ebola in Western Africa (Constantine and Howard, 2016; Diaz et al., 2018). The SEIR model is a type of compartmental model used in epidemiology to simulate how diseases spread through a population. It's an extension of the basic SIR model, which stands for Susceptible, Infected, and Recovered compartments. The SEIR model adds an additional compartment, Exposed (E), to account for a latency period between when an individual is exposed to a disease and when they become infectious. For this example, we have access to a computational model and its gradients so we can compute the true expected outer product matrix in order to identify the relevant feature subspace following a similar setup as in Section 5. As the results are similar to the simulation studies, we refer the reader to Appendix E.2 for the data generation model and the detailed results on the performance of our proposed TrIM method.

Next, we focus on the empirical performance of our proposed method on real data applications, against other popular dimension reduction methods combined with Random Forests. We consider the following datasets from the UCI Machine Learning Repository (Dua and Graff, 2019) and OpenML (Vanschoren et al., 2014), which represent a variety of regression tasks on real-valued covariates:

Dataset	# of samples, n	# of features, d
Abalone	4177	8
Auto Price	159	15
Diabetes	768	8
Mu284	284	9
Bank8FM	8192	8
Kin8nm	8192	8

The Abalone dataset contains physical measurements of abalones, a type of marine snail, and the number of rings on the shell, which is used to estimate the age of the abalone. The Auto Price dataset contains information about cars and their prices. The Diabetes dataset contains information about diabetes patients. The Mu284 dataset contains information about the energy of molecules. The Bank8FM dataset contains information about bank customers. The Kin8nm dataset contains information about the energy of molecules. For these datasets, we do not have access to the true relevant feature subspace, so we compare the performance of the proposed iterative method with the baseline Mondrian forest and other state-of-the-art random forest methods.

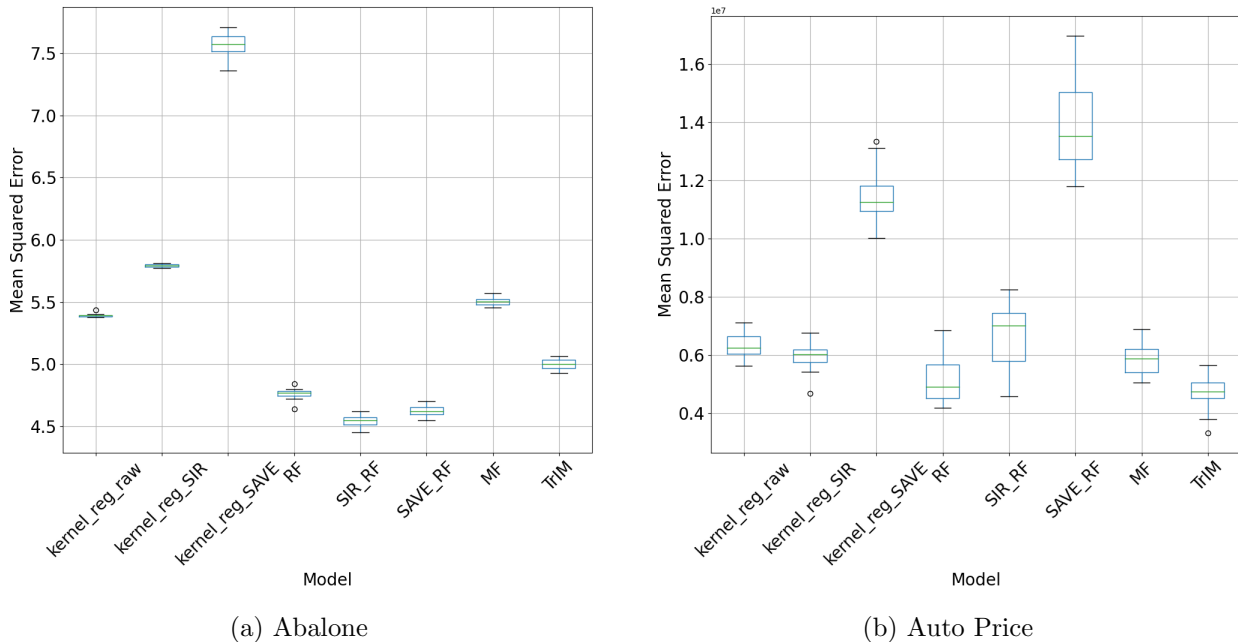


Fig 5: Comparison of the test mean squared error (MSE) of different methods for real data applications, where the box plot displays the variation across 15 trials. Similar patterns are observed across more datasets, which are presented in Figure 10 in Appendix E.3.

We compare **TrIM** with the Mondrian forest baseline (MF) and two popular options: traditional Breiman random forests (RF) (Breiman, 2001) and Nadaraya-Watson kernel estimators (NW Kernel) (Nadaraya, 1964; Watson, 1964). We also include two variations on the traditional random forest (SIR + RF and SAVE + RF) and the Nadaraya-Watson kernel estimator (SIR + NW Kernel and SAVE + NW Kernel). As their names suggest, these two variants first extract predictors using SIR or SAVE, and then train a random forest or a Nadaraya-Watson kernel estimator using only these features. This approach of using global dimension reduction predictors within a kernel estimator is common practice, see Adraghi and Cook (2009). We use the Python package `scikit-learn` for the

traditional random forests and the code from [Loyal et al. \(2022\)](#) for the other methods.¹

For every dataset, we conduct a 10-fold cross-validation procedure. This involved dividing the dataset into 10 equal parts, training our models on 9 parts, and testing them on the remaining part. This process was repeated 10 times, each time with a different part used as the test set, to ensure thorough evaluation. After completing these cycles, we calculated the mean squared error (MSE) for the predictions made on the test sets across all 10 folds to assess the models' out-of-sample performance. The cross-validation procedure was repeated 15 times to construct the box-plots shown in [Figure 5](#).

For all methods, we used $M = 10$ trees for constructing the random forest and applied a default grid search strategy, which systematically explored various combinations of hyperparameters and choose the best possible model found among all hyperparameter choices using the training set. Then we evaluate the performance of the chosen models on the test set. For methods involving the traditional random forest, the specific hyperparameters we focused on were `min_samples_leaf` and `max_features`. For `min_samples_leaf`, we evaluated both 1 and 5 as potential values. Meanwhile, for `max_features`, we considered a range of options: 2, 4, 6, a third of the features (expressed as $1/3$), the square root of the number of features (`sqrt`), and the option to use all features (`None`). For both Mondrian forest methods (MF and `TrIM`), we choose the lifetime parameter $\lambda \in \{1, 2, 3, 4, 5\}$. For our proposed method (`TrIM`), we set the maximum number of iterations $T = 2$ and the step size $t \in \{0.1, 0.2, 0.5\}$.

[Figure 5](#) presents the results of our real data experiment: each data point in the plot represents the average MSE across the 10 test folds in cross-validation, and each box shows the variation of the average MSE across 15 random trials of the cross-validation procedure. Our proposed method consistently outperforms the baseline Mondrian forest across all datasets. The proposed method is also competitive against the other methods. The results suggest that `TrIM` can effectively identify the relevant feature subspace and leverage this knowledge to improve predictive performance of Mondrian forests on real data applications.

7. Conclusion and Future Directions

In this work, we propose a new iterative random forest algorithm (`TrIM`) that is competitive with state-of-the-art methods and adaptive to low-dimensional structure in the regression function captured by the linear dimension reduction model known as a ridge function, or multi-index model. Convergence rates for the estimator after one iteration of the algorithm are also obtained that account for the estimation error in the relevant feature subspace. In future work we will obtain guarantees that take into account multiple steps of the iterative approach, quantifying the improvement in the rate with multiple iterations.

Other future directions include studying different variants of sufficient dimension reduction and active subspace learning techniques and incorporating them into the computationally efficient and theoretically amenable framework of Mondrian forest prediction. For example, one can consider the setting of sparse sufficient dimension reduction ([Lu Li and Yu, 2020](#)), where the relevant feature subspace is assumed to be spanned by a set of sparse vectors consisting of linear combinations of a small number of covariates, a setting that increases the interpretability of the model and is relevant in many applications. Another direction is to study nonlinear dimension reduction mechanisms. Indeed, the linear dimension reduction methods considered in this paper are limited to finding *globally* relevant features. While they have been successful in several applications, the data may exhibit

¹We were unable, however, to reproduce the Dimension Reduction Forest introduced in [Loyal et al. \(2022\)](#) due to an incompatibility of the `Cython` package used in their code.

locally relevant features that are not captured by linear features. Nonlinear dimension reduction has also been considered in the sufficient dimension reduction literature (Wu, 2008; Lee et al., 2013) and from the gradient-based perspective (Bigoni et al., 2022) in active subspace learning, but has not yet been combined with random forest prediction.

Acknowledgments

The authors thank the High Performance Computing Center (HPCC) at the Wharton School, University of Pennsylvania for providing computational resources that supported the experimental results presented in this paper. The authors would also like to extend their gratitude to Ngoc Mai Tran for her valuable suggestions regarding the methodology of this study. RB is grateful for support from the von Kármán instructorship at Caltech and a Department of Defense (DoD) Vannevar Bush Faculty Fellowship (award N00014-22-1-2790) held by Andrew M. Stuart.

References

- Kofi P Adraghi and R Dennis Cook. Sufficient dimension reduction and prediction in regression. *Philosophical Transactions of the Royal Society A: Mathematical, Physical and Engineering Sciences*, 367(1906):4385–4405, 2009.
- Abhineet Agarwal, Ana M. Kenney, Yan Shuo Tan, Tiffany M. Tang, and Bin Yu. MDI+: A flexible random forest-based feature importance framework. *arXiv:2307.01932*, 2023.
- Matej Balog, Balaji Lakshminarayanan, Zoubin Ghahramani, Daniel M Roy, and Yee Whye Teh. The Mondrian kernel. In *Proceedings of the Thirty-Second Conference on Uncertainty in Artificial Intelligence*, pages 32–41, 2016.
- Sumanta Basu, Karl Kumbier, James B Brown, and Bin Yu. Iterative random forests to discover predictive and stable high-order interactions. *Proceedings of the National Academy of Sciences*, 115(8):1943–1948, 2018.
- Daniele Bigoni, Youssef Marzouk, Clémentine Prieur, and Olivier Zahm. Nonlinear dimension reduction for surrogate modeling using gradient information. *Information and Inference: A Journal of the IMA*, 11(4), 2022.
- James Bradbury, Roy Frostig, Peter Hawkins, Matthew James Johnson, Chris Leary, Dougal Maclaurin, George Necula, Adam Paszke, Jake VanderPlas, Skye Wanderman-Milne, et al. JAX: Composable transformations of Python+NumPy programs. <https://github.com/google/jax>, 2018.
- Leo Breiman. Random forests. *Machine learning*, 45(1):5–32, 2001.
- Clément Bénard, Sébastien Da Veiga, and Erwan Scornet. Mean decrease accuracy for random forests: inconsistency, and a practical solution via the Sobol-MDA. *Biometrika*, 109(4):881–900, December 2022.
- Matias D. Cattaneo, Jason M. Klusowski, and William G. Underwood. Inference with Mondrian random forests. *arXiv:2310.09702*, 2023.
- Tim Coleman, Wei Peng, and Lucas Mentch. Scalable and efficient hypothesis testing with random forests. *Journal of Machine Learning Research*, 23:1–35, 2022.
- Paul Constantine and Ryan Howard. Active Subspace data sets. <https://github.com/paulcon/as-data-sets>, 2016.
- Paul G Constantine, Eric Dow, and Qiqi Wang. Active subspace methods in theory and practice:

- applications to kriging surfaces. *SIAM Journal on Scientific Computing*, 36(4):A1500–A1524, 2014.
- R. Dennis Cook. Fisher Lecture: Dimension Reduction in Regression. *Statistical Science*, 22(1):1 – 26, 2007.
- Wenying Deng, Beau Coker, Rajarshi Mukherjee, Jeremiah Zhe Liu, and Brent A. Coull. Towards a unified framework for uncertainty-aware nonlinear variable selection with theoretical guarantees. In Alice H. Oh, Alekh Agarwal, Danielle Belgrave, and Kyunghyun Cho, editors, *Advances in Neural Information Processing Systems*, 2022.
- R Dennis Cook. SAVE: A method for dimension reduction and graphics in regression. *Communications in statistics-Theory and methods*, 29(9-10):2109–2121, 2000.
- Paul Diaz, Paul Constantine, Kelsey Kalmbach, Eric Jones, and Stephen Pankavich. A modified SEIR model for the spread of Ebola in Western Africa and metrics for resource allocation. *Applied mathematics and computation*, 324:141–155, 2018.
- Dheeru Dua and Casey Graff. UCI machine learning repository. <http://archive.ics.uci.edu/ml>, 2019.
- Manuel Fernández-Delgado, Eva Cernadas, Senén Barro, and Dinani Amorim. Do we need hundreds of classifiers to solve real world classification problems? *The journal of machine learning research*, 15(1):3133–3181, 2014.
- Shufei Ge, Shijia Wang, Yee Whye Teh, Liangliang Wang, and Lloyd Elliott. Random tessellation forests. *Advances in Neural Information Processing Systems*, 32, 2019.
- László Györfi, Michael Kohler, Adam Krzyzak, and Harro Walk. *A Distribution-Free Theory of Nonparametric Regression*. Springer, 2002.
- Trevor Hastie, Robert Tibshirani, Jerome H Friedman, and Jerome H Friedman. *The elements of statistical learning: data mining, inference, and prediction*, volume 2. Springer, 2009.
- Giles Hooker, Lucas Mentch, and Siyu Zhou. Unrestricted permutation forces extrapolation: variable importance requires at least one more model, or there is no free variable importance. *Statistics and Computing*, 31(82), 2021.
- Balaji Lakshminarayanan, Daniel M Roy, and Yee Whye Teh. Mondrian forests: Efficient online random forests. In *Advances in neural information processing systems*, pages 3140–3148, 2014.
- Balaji Lakshminarayanan, Daniel M Roy, and Yee Whye Teh. Mondrian forests for large-scale regression when uncertainty matters. In *Artificial Intelligence and Statistics*, pages 1478–1487, 2016.
- Kuang-Yao Lee, Bing Li, and Francesca Chiaromonte. A general theory for nonlinear sufficient dimension reduction: Formulation and estimation. *The Annals of Statistics*, 41(1):221–249, 2013.
- B. Li. *Sufficient Dimension Reduction: Methods and Applications with R (1st ed.)*. Chapman and Hall/CRC, 2017.
- Ker-Chau Li. Sliced inverse regression for dimension reduction. *Journal of the American Statistical Association*, 86(414):316–327, 1991.
- Qian Lin, Zhigen Zhao, and Jun S. Liu. On consistency and sparsity for sliced inverse regression in high dimensions. *The Annals of Statistics*, 46(2):580–610, 2018.
- Joshua Daniel Loyal, Ruoqing Zhu, Yifan Cui, and Xin Zhang. Dimension reduction forests: Local variable importance using structured random forests. *Journal of Computational and Graphical Statistics*, 31(4):1104–1113, 2022.
- Xuerong Meggie Wen Lu Li and Zhou Yu. A selective overview of sparse sufficient dimension

- reduction. *Statistical Theory and Related Fields*, 2020.
- Scott M. Lundberg, Gabriel Erion, Hugh Chen, Alex DeGrave, Jordan M. Prutkin, Bala Nair, Ronit Katz, Jonathan Himmelfarb, Nisha Bansal, and Su-In Lee. From local explanations to global understanding with explainable ai for trees. *Nature Machine Intelligence volume*, 2:56–67, 2020.
- Jaouad Mourtada, Stéphane Gaïffas, and Erwan Scornet. Minimax optimal rates for Mondrian trees and forests. *Annals of Statistics*, 28(4):2253–2276, 2020.
- Elizbar A Nadaraya. On estimating regression. *Theory of Probability & Its Applications*, 9(1): 141–142, 1964.
- Werner Nagel and Viola Weiss. Crack STIT tessellations: Characterization of stationary random tessellations stable with respect to iteration. *Advances in Applied Probability*, 37:859–883, 2005.
- Eliza O'Reilly. Statistical advantages of oblique randomized decision trees and forests. *arXiv:2407.02458*, 2024.
- Eliza O'Reilly and Ngoc Mai Tran. Stochastic geometry to generalize the Mondrian process. *SIAM Journal on Mathematics of Data Science*, 4(2):531–552, 2022.
- Eliza O'Reilly and Ngoc Mai Tran. Minimax rates for high-dimensional random tessellation forests. *Journal of Machine Learning Research*, 25:1–32, 2024.
- Allan Pinkus. *Ridge functions*, volume 205. Cambridge University Press, 2015.
- Adityanarayanan Radhakrishnan, Daniel Beaglehole, Parthe Pandit, and Mikhail Belkin. Mechanism of feature learning in deep fully connected networks and kernel machines that recursively learn features. *arXiv:2212.13881*, 2023.
- Daniel M Roy and Yee Whye Teh. The Mondrian process. In *Proceedings of the 21st International Conference on Neural Information Processing Systems*, pages 1377–1384, 2008.
- Rolf Schneider and Wolfgang Weil. *Stochastic and Integral Geometry*. Probability and Its Applications. Springer-Verlag, Berlin, 2008.
- Carolina Strobl, Anne-Laure Boulesteix, Achim Zeileis, and Torsten Hothorn. Bias in random forest variable importance measures: Illustrations, sources and a solution. *BMC Bioinformatics*, 8(1), January 2007.
- Carolina Strobl, Anne-Laure Boulesteix, Thomas Kneib, Thomas Augustin, and Achim Zeileis. Conditional variable importance for random forests. *BMC Bioinformatics*, 9(307), 2008.
- Shubhendu Trivedi, Jialei Wang, Samory Kpotufe, and Gregory Shakhnarovich. A consistent estimator of the expected gradient outerproduct. In *Uncertainty in Artificial Intelligence - Proceedings of the 30th Conference, UAI 2014*, pages 819–828. AUAI Press, 2014.
- Joel A Tropp. User-friendly tail bounds for sums of random matrices. *Foundations of computational mathematics*, 12:389–434, 2012.
- Joaquin Vanschoren, Jan N Van Rijn, Bernd Bischl, Luís Torgo, Bernd Bischl, Jana Kietz, Jan N van Rijn, Bernd Bischl, Luís Torgo, Bernd Bischl, Jana Kietz, et al. OpenML: networked science in machine learning. *ACM SIGKDD Explorations Newsletter*, 15(2):49–60, 2014.
- Geoffrey S Watson. Smooth regression analysis. *Sankhyā: The Indian Journal of Statistics, Series A*, pages 359–372, 1964.
- Han-Ming Wu. Kernel sliced inverse regression with applications to classification. *Journal of Computational and Graphical Statistics*, 17(3):590–610, 2008.
- Yingcun Xia, Howell Tong, Wai Keung Li, and Li-Xing Zhu. An adaptive estimation of dimension reduction space. *Journal of the Royal Statistical Society: Series B (Statistical Methodology)*, 64

(3):363–410, 2002.

Ke Ye and Lek-Heng Lim. Schubert varieties and distances between subspaces of different dimensions. *SIAM Journal on Matrix Analysis and Applications*, 37(3):1176–1197, 2016.

Olivier Zahm, Paul G Constantine, Clémentine Prieur, and Youssef M Marzouk. Gradient-based dimension reduction of multivariate vector-valued functions. *SIAM Journal on Scientific Computing*, 42(1):A534–A558, 2020.

Ruoqing Zhu, Donglin Zeng, and Michael R Kosorok. Reinforcement learning trees. *Journal of the American Statistical Association*, 110(512):1770–1784, 2015.

Appendix A: Approximation of Gradient Outer Product: Proof of Theorem 4 and Corollary 5

We first consider the proof of the estimation error rate of the estimator $\widehat{H}_n := \widehat{H}_{n,t}$ as defined in (8) of the expected gradient outer product H given by (5). Throughout, we will denote by \mathbb{E}_Y the expectation taken with respect to a random variable Y .

A.1. Risk Bound for Shifted Input

A core lemma to control the error of the gradient estimator is a risk bound for the Mondrian forest estimator with a shift input. This proof follows closely that of the proofs of Theorem 3 in Mourtada et al. (2020) and Theorem 6 in O'Reilly and Tran (2024) but must take into account the fact the the input could lie outside of the support of the input data used to train the forest estimator.

Lemma 12. *Suppose f satisfies Assumption 3 and the distribution μ of the random input X satisfies Assumption 2. Fix $t \geq 0$. For $s \in \{-t, t\}$ and $j \in [d]$, there exists a constant c_μ just depending on μ such that*

$$\begin{aligned} \mathbb{E} \left[(f(X + se_j) - \widehat{f}_{\lambda,n,M}(X + se_j))^2 \right] &\leq \tilde{c}_\mu \left[\frac{L^2 d^8}{\lambda^4} + \frac{L^2 d^6}{\lambda^3} \sum_{k=1}^d \binom{d}{k} \frac{2^k d^{2k} \kappa_k}{\lambda^k} \right. \\ &\quad \left. + \frac{L^2 d^4}{\lambda^2} \sum_{k=1}^d \binom{d}{k} \frac{2^k d^{2k} \kappa_k}{\lambda^k} + \frac{L^2}{\lambda^2 M d} + \frac{(5\|f\|_\infty^2 + 2\sigma^2)}{n} (1 + \lambda)^d (1 + t)^d \right]. \end{aligned}$$

As $n \rightarrow \infty$, assuming $\lambda, M \rightarrow \infty$ and $t \rightarrow 0$, the asymptotic behavior of the upper bound satisfies

$$\mathbb{E} \left[(f(X + se_j) - \widehat{f}_{\lambda,n,M}(X + se_j))^2 \right] \lesssim \frac{\lambda^d}{n} + \frac{L^2}{\lambda^3} + \frac{L^2}{\lambda^2 M}.$$

Remark 1. The asymptotic bound can be improved to $\frac{\lambda^d}{n} + \frac{L^2}{\lambda^4} + \frac{L^2}{\lambda^2 M}$ if we condition on X begin at least distance $d(X, \partial K) \geq \varepsilon > 0$ away from the boundary of the support K of μ , similarly to the risk bound for \mathcal{C}^2 functions in Mourtada et al. (2020) and O'Reilly and Tran (2024).

Proof. We proceed as in the proof of Theorem 3 in Mourtada et al. (2020) by decomposing the risk of the forest estimator into bias and variance terms:

$$\mathbb{E}[(\widehat{f}_{\lambda,n,M}(X) - f(X))^2] = \mathbb{E}[(f(X) - \bar{f}_{\lambda,M}(X))^2] + \mathbb{E}[(\bar{f}_{\lambda,M}(X) - \widehat{f}_{\lambda,n,M}(X))^2], \quad (13)$$

where we define for each m and $x \in \mathbb{R}^d$,

$$\bar{f}_\lambda^{(m)}(x) := \mathbb{E}_X[f(X) | X \in Z_x^{\lambda,(m)}],$$

and $\bar{f}_{\lambda,M}(x) := \frac{1}{M} \sum_{m=1}^M \bar{f}_{\lambda}^{(m)}(x)$.

We first consider the variance term, and condition on the Mondrian tessellation $\mathcal{P}(\lambda)$ with lifetime λ to obtain the variance of the tree estimator corresponding to a fixed tessellation. Note that the assumption \mathcal{D}_n and $\mathcal{P}(\lambda)$ are independent allows us to take the expectations separately. Also, recall that if no points of $\{X_1, \dots, X_n\}$ fall in Z_x^λ , then $\hat{f}_{\lambda,n}(x) = 0$. For each $C \in \mathcal{P}(\lambda)$, let $\mathcal{N}_n(C) = \sum_{i=1}^n \mathbf{1}_{\{X_i \in C\}}$ be the number of covariates inside C and let $p_{\lambda,C} := \mathbb{P}_X(X \in C)$. Then,

$$\begin{aligned} \mathbb{E}_{\mathcal{D}_n} \left[(\bar{f}_{\lambda}(x) - \hat{f}_{\lambda,n}(x))^2 \right] &= \sum_{\substack{C \in \mathcal{P}(\lambda): \\ C \cap K \neq \emptyset}} \mathbf{1}_{\{x \in C\}} \mathbb{E}_{\mathcal{D}_n} \left[\left(\mathbb{E}_X[f(X)|X \in C] - \frac{\sum_{i=1}^n Y_i \mathbf{1}_{\{X_i \in C\}}}{\mathcal{N}_n(C)} \right)^2 \right] \\ &= \sum_{\substack{C \in \mathcal{P}(\lambda): \\ C \cap K \neq \emptyset}} \mathbf{1}_{\{x \in C\}} \mathbb{E}_{\mathcal{D}_n} \left[\left(\mathbb{E}_X[f(X)|X \in C] - \frac{\sum_{i=1}^n Y_i \mathbf{1}_{\{X_i \in C\}}}{\mathcal{N}_n(C)} \right)^2 \right]. \end{aligned}$$

From the proof of Lemma 20 in O'Reilly and Tran (2024), the expectation in the sum satisfies

$$\begin{aligned} &\mathbb{E}_{\mathcal{D}_n} \left[\left(\mathbb{E}_X[f(X)|X \in C] - \frac{\sum_{i=1}^n Y_i \mathbf{1}_{\{X_i \in C\}}}{\mathcal{N}_n(C)} \right)^2 \right] \\ &\leq (2\|f\|_\infty^2 + \sigma^2) \sum_{k=1}^n \binom{n}{k} p_{\lambda,C}^k (1 - p_{\lambda,C})^{n-k} k^{-1} + \|f\|_\infty^2 (1 - p_{\lambda,C})^n. \end{aligned}$$

Now, note that for $B \sim \text{Binomial}(n, p_{\lambda,C})$,

$$\sum_{k=1}^n \binom{n}{k} n p_{\lambda,C}^{k+1} (1 - p_{\lambda,C})^{n-k} k^{-1} = \mathbb{E}[B] \mathbb{E}[B^{-1} \mathbf{1}_{\{B > 0\}}],$$

and $\mathbb{E}[B] \mathbb{E}[B^{-1} \mathbf{1}_{\{B > 0\}}] \leq \frac{2np_{\lambda,C}}{(n+1)p_{\lambda,C}} \leq 2$ (Györfi et al., 2002, Lemma 4.1). Also, the upper bounds $1 - x \leq e^{-x}$ and $xe^{-x} \leq e^{-1}$ for all $x \geq 0$ imply

$$np_{\lambda,C}(1 - p_{\lambda,C})^n \leq e^{-1} \leq 1.$$

Thus we have the pointwise upper bound

$$\begin{aligned} \mathbb{E}_{\mathcal{D}_n} \left[(\bar{f}_{\lambda}(x) - \hat{f}_{\lambda,n}(x))^2 \right] &\leq \frac{1}{n} \sum_{\substack{C \in \mathcal{P}(\lambda): \\ C \cap K \neq \emptyset}} \mathbf{1}_{\{x \in C\}} (2\|f\|_\infty^2 + \sigma^2) \sum_{k=1}^n \binom{n}{k} n p_{\lambda,C}^k (1 - p_{\lambda,C})^{n-k} k^{-1} \\ &\quad + \frac{\|f\|_\infty^2}{n} \sum_{\substack{C \in \mathcal{P}(\lambda): \\ C \cap K \neq \emptyset}} n \mathbf{1}_{\{x \in C\}} (1 - p_{\lambda,C})^n \\ &\leq \frac{(2\|f\|_\infty^2 + \sigma^2)}{n} \sum_{\substack{C \in \mathcal{P}(\lambda): \\ C \cap K \neq \emptyset}} \mathbf{1}_{\{x \in C\}} p_{\lambda,C}^{-1} + \frac{\|f\|_\infty^2}{n} \sum_{\substack{C \in \mathcal{P}(\lambda): \\ C \cap K \neq \emptyset}} \mathbf{1}_{\{x \in C\}} p_{\lambda,C}^{-1} \\ &\leq \frac{5\|f\|_\infty^2 + 2\sigma^2}{n} \sum_{\substack{C \in \mathcal{P}(\lambda): \\ C \cap K \neq \emptyset}} \mathbf{1}_{\{x \in C\}} p_{\lambda,C}^{-1}. \end{aligned}$$

Now, note that for $t \geq 0$ the support of $X + te_j$ is contained in $(1+t)K$ since $K = [0, 1]^d$. Taking the expectation with respect to the shifted input gives

$$\begin{aligned} & \mathbb{E}_X \left[\mathbb{E}_{\mathcal{D}_n} \left[(\bar{f}_\lambda(X + te_j) - \hat{f}_{\lambda,n}(X + te_j))^2 \right] \right] \\ & \leq \frac{5\|f\|_\infty^2 + 2\sigma^2}{n} \sum_{\substack{C \in \mathcal{P}(\lambda): \\ C \cap K \neq \emptyset}} \mathbb{P}(X + te_j \in C) p_{\lambda,C}^{-1} \\ & \leq \frac{(5\|f\|_\infty^2 + 2\sigma^2)p_1}{np_0} \sum_{C \in \mathcal{P}(\lambda)} \text{vol}_d((1+t)K \cap C) \text{vol}_d(K \cap C)^{-1} \\ & \leq \frac{(5\|f\|_\infty^2 + 2\sigma^2)p_1}{np_0} N_\lambda(K) (1+t)^d. \end{aligned}$$

Finally, taking the expectation with respect to \mathcal{P} and using Lemma 6 in O'Reilly and Tran (2024), we have,

$$\mathbb{E} \left[(\bar{f}_\lambda(X + te_j) - \hat{f}_{\lambda,n}(X + te_j))^2 \right] \leq \frac{(5\|f\|_\infty^2 + 2\sigma^2)p_1}{np_0} (1+\lambda)^d (1+t)^d.$$

A similar argument gives

$$\mathbb{E} \left[(\bar{f}_\lambda(X - te_j) - \hat{f}_{\lambda,n}(X - te_j))^2 \right] \leq \frac{(5\|f\|_\infty^2 + 2\sigma^2)p_1}{np_0} (1+\lambda)^d (1+t)^d.$$

We now turn to bounding the bias term. For $x \in \mathbb{R}^d$, define

$$\tilde{f}_\lambda(x) = \mathbb{E}_{\mathcal{P}}[\bar{f}_\lambda(x)] = \mathbb{E} \left[\frac{1}{\mu(Z_x^\lambda)} \int_{Z_x^\lambda} f(y) d\mu(x) \right].$$

From the proof of Theorem 13 in O'Reilly and Tran (2024),

$$\mathbb{E}_{\mathcal{P}} [|f(x) - \bar{f}_\lambda(x)|^2] \leq \mathbb{E}_{\mathcal{P}} [|f(x) - \tilde{f}_\lambda(x)|^2] + \frac{L^2 \mathbb{E}[\mathbb{D}(Z_0)^2]}{\lambda^2 M},$$

and for a constant c_μ depending only on μ ,

$$\mathbb{E}[(f(x) - \tilde{f}_\lambda(x))^2] \leq c_\mu \left(\frac{L \mathbb{E}[\mathbb{D}(Z_0)^2]}{\lambda^2} + \frac{L}{\lambda} \mathbb{E} \left[\mathbb{D}(Z_0) \frac{\text{vol}(Z_0 \cap \lambda(K^c - x))}{\text{vol}(Z_0)} \right] \right)^2.$$

Then,

$$\begin{aligned} & \mathbb{E}[(f(x) - \tilde{f}_\lambda(x))^2] \\ & \leq \frac{c_\mu L^2}{\lambda^4} \mathbb{E}[\mathbb{D}(Z_0)^2]^2 + \frac{2c_\mu L^2}{\lambda^3} \mathbb{E}[\mathbb{D}(Z_0)^2] \mathbb{E} \left[\mathbb{D}(Z_0) \frac{\text{vol}(Z_0 \cap \lambda(K^c - x))}{\text{vol}(Z_0)} \right] \\ & \quad + \frac{c_\mu L^2}{\lambda^2} \mathbb{E} \left[\mathbb{D}(Z_0) \frac{\text{vol}(Z_0 \cap \lambda(K^c - x))}{\text{vol}(Z_0)} \right]^2, \end{aligned}$$

and taking the expectation with respect to the shift input X gives for $s \in \{-t, t\}$,

$$\begin{aligned}
& \mathbb{E}[(f(X + se_j) - \tilde{f}_\lambda(X + se_j))^2] \\
& \leq \frac{c_\mu L^2}{\lambda^4} \mathbb{E}[D(Z_0)^2]^2 + \frac{2c_\mu L^2}{\lambda^3} \mathbb{E}[D(Z_0)^2] \mathbb{E}\left[D(Z_0) \frac{\text{vol}(Z_0 \cap \lambda(K^c - X - se_j))}{\text{vol}(Z_0)}\right] \\
& \quad + \frac{c_\mu L^2}{\lambda^2} \mathbb{E}_X \left[\mathbb{E}_{\mathcal{P}} \left[D(Z_0) \frac{\text{vol}(Z_0 \cap \lambda(K^c - X - se_j))}{\text{vol}(Z_0)} \right]^2 \right] \\
& \leq \frac{c_\mu L^2}{\lambda^4} \mathbb{E}[D(Z_0)^2]^2 + \frac{2c_\mu L^2}{\lambda^3} \mathbb{E}[D(Z_0)^2] \mathbb{E}\left[D(Z_0) \frac{\text{vol}(Z_0 \cap \lambda(K^c - X - se_j))}{\text{vol}(Z_0)}\right] \\
& \quad + \frac{c_\mu L^2}{\lambda^2} \mathbb{E}[D(Z_0)] \mathbb{E}\left[D(Z_0) \frac{\text{vol}(Z_0 \cap \lambda(K^c - X - se_j))}{\text{vol}(Z_0)}\right].
\end{aligned}$$

Next, we see that for $s \in \{-t, t\}$,

$$\begin{aligned}
\mathbb{E}_X[\text{vol}_d(Z_0 \cap \lambda(K^c - X - se_j))] &= \int_K p(x) \left(\int_{\mathbb{R}^d} 1_{\{y \in Z_0 \cap \lambda(K^c - x - se_j)\}} dy \right) dx \\
&\leq p_1 \int_K \int_{\mathbb{R}^d} 1_{\{y \in Z_0 + se_j \cap \lambda(K^c - x)\}} dy dx \\
&= p_1 \int_{Z_0 + se_j} \int_K 1_{\{x \in K^c - \frac{y}{\lambda}\}} dx dy \\
&= p_1 \int_{Z_0 + se_j} \text{vol}_d\left(K \cap K^c - \frac{y}{\lambda}\right) dy \\
&= p_1 \int_{Z_0 + se_j} \text{vol}_d\left(K \cup K - \frac{y}{\lambda}\right) dy - p_1 \text{vol}_d(Z_0) \text{vol}_d(K),
\end{aligned}$$

where we have used that $\text{vol}_d(K \cap K^c - y/\lambda) = \text{vol}_d(K) - \text{vol}_d(K \cap K - y/\lambda)$ and $\text{vol}_d(K \cap K - y/\lambda) = 2\text{vol}_d(K) - \text{vol}_d(K \cup K - y/\lambda)$. We now observe that the union $K \cup K - \frac{y}{\lambda}$ is a subset of the Minkowski sum $K + \frac{\|y\|}{\lambda} B^d$. By Steiner's formula ([Schneider and Weil, 2008](#), Equation (14.5)),

$$\begin{aligned}
\text{vol}_d\left(K \cup K - \frac{y}{\lambda}\right) &\leq \text{vol}_d\left(K + \frac{\|y\|}{\lambda} B^d\right) = \sum_{j=0}^d \left(\frac{\|y\|}{\lambda}\right)^{d-j} \kappa_{d-j} V_j(K) \\
&= \text{vol}_d(K) + \sum_{j=0}^{d-1} \left(\frac{\|y\|}{\lambda}\right)^{d-j} \kappa_{d-j} V_j(K).
\end{aligned}$$

The intrinsic volumes $V_j(K)$ for the unit cube $K = [0, 1]^d$ satisfy $V_j([0, 1]^d) = \binom{d}{j}$ for each $j = 1, \dots, d$. Thus,

$$\begin{aligned}
\mathbb{E}_X[\text{vol}_d(Z_0 \cap \lambda(K^c - X - se_j))] &\leq p_1 \text{vol}_d(Z_0) \sum_{j=0}^{d-1} \binom{d}{j} \left(\frac{D(Z_0 + se_j)}{\lambda}\right)^{d-j} \kappa_{d-j} \\
&\leq p_1 \text{vol}_d(Z_0) \sum_{j=0}^{d-1} \binom{d}{j} \frac{D(Z_0)^{d-j} \kappa_{d-j}}{\lambda^{d-j}} \\
&= p_1 \text{vol}_d(Z_0) \sum_{k=1}^d \binom{d}{k} \frac{D(Z_0)^k \kappa_k}{\lambda^k},
\end{aligned}$$

and

$$\mathbb{E} \left[\frac{\mathbb{D}(Z_0) \text{vol}_d(Z_0 \cap \lambda(K^c - X - se_j))}{\text{vol}_d(Z_0)} \right] \leq p_1 \sum_{k=1}^d \binom{d}{k} \frac{\mathbb{E}[\mathbb{D}(Z_0)^{k+1}] \kappa_k}{\lambda^k}.$$

Thus,

$$\begin{aligned} & \mathbb{E} (|f(X + se_j) - \bar{f}_\lambda(X + se_j)|^2) \\ & \leq \frac{c_\mu L^2 \mathbb{E} [\mathbb{D}(Z_0)^2]^2}{\lambda^4} + \frac{2c_\mu L^2 p_1 \mathbb{E} [\mathbb{D}(Z_0)^2]}{\lambda^3} \sum_{k=1}^d \binom{d}{k} \frac{\mathbb{E}[\mathbb{D}(Z_0)^{k+1}] \kappa_k}{\lambda^k} \\ & \quad + \frac{c_\mu L^2 p_1 \mathbb{E}[\mathbb{D}(Z_0)]}{\lambda^2} \sum_{k=1}^d \binom{d}{k} \frac{\mathbb{E}[\mathbb{D}(Z_0)^{k+1}] \kappa_k}{\lambda^k} + \frac{L^2 \mathbb{E}[\mathbb{D}(Z_0)^2]}{\lambda^2 M}, \end{aligned}$$

Finally by Lemma 24 from O'Reilly (2024), for $k > 0$,

$$\mathbb{E} [\mathbb{D}(Z_0)^{k+1}] \leq \frac{\Gamma(2d + k + 1) d^{k+1}}{\Gamma(2d)} \leq 2^{k+1} d^{2k+2},$$

and

$$\begin{aligned} \mathbb{E} (|f(X + se_j) - \bar{f}_\lambda(X + se_j)|^2) & \leq \frac{16c_\mu L^2 d^8}{\lambda^4} + \frac{8c_\mu L^2 p_1 d^4}{\lambda^3} \sum_{k=1}^d \binom{d}{k} \frac{2^{k+1} d^{2k+2} \kappa_k}{\lambda^k} \\ & \quad + \frac{2c_\mu L^2 p_1 d^2}{\lambda^2} \sum_{k=1}^d \binom{d}{k} \frac{2^{k+1} d^{2k+2} \kappa_k}{\lambda^k} + \frac{4L^2 d^4}{\lambda^2 M}, \end{aligned}$$

Combining the bias and variance bounds gives that there exists a constant \tilde{c}_μ depending only on μ such that

$$\begin{aligned} \mathbb{E} \left[(f(X + se_j) - \hat{f}_{\lambda, n, M}(X + se_j))^2 \right] & \leq \tilde{c}_\mu \left[\frac{L^2 d^8}{\lambda^4} + \frac{L^2 d^6}{\lambda^3} \sum_{k=1}^d \binom{d}{k} \frac{2^k d^{2k} \kappa_k}{\lambda^k} \right. \\ & \quad \left. + \frac{L^2 d^4}{\lambda^2} \sum_{k=1}^d \binom{d}{k} \frac{2^k d^{2k} \kappa_k}{\lambda^k} + \frac{L^2}{\lambda^2 M d} + \frac{(5\|f\|_\infty^2 + 2\sigma^2)}{n} (1 + \lambda)^d (1 + t)^d \right]. \end{aligned}$$

□

A.2. Gradient estimation error

Proposition 13. Assume μ and f satisfy Assumptions 2 and 3. Let $\hat{f}_n = \hat{f}_{n, \lambda, M}$ be a Mondrian forest estimator of f . As $n \rightarrow \infty$ assuming $\lambda, M \rightarrow \infty$ and $t \rightarrow 0$,

$$\mathbb{E} \left[\|\nabla f(X) - \widehat{\nabla} \hat{f}_n(X)\|_2^2 \right] \lesssim \frac{1}{t^2} \left(\frac{\lambda^d}{n} + \frac{L^2}{\lambda^3} + \frac{L^2}{\lambda^2 M} \right) + L^2 t^2,$$

where the expectation is taken with respect to X, \mathcal{D}_n , and \mathcal{P} . Then, letting $\lambda \sim n^{\frac{1}{d+3}}$, $M \gtrsim n^{\frac{1}{d+3}}$ and $t \sim n^{-\frac{3}{4d+12}}$ gives

$$\mathbb{E} [\|\widehat{\nabla} \hat{f}_n(X) - \nabla f(X)\|_2^2] \lesssim n^{-\frac{3}{2d+6}}.$$

Proof. Now, as in Section 4.1 of [Trivedi et al. \(2014\)](#) define the vector

$$\widehat{\nabla} f(x) := (\Delta_{i,t} f(x) \cdot \mathbf{1}_{E_{n,i}(x)})_{i \in [d]}.$$

By the triangle inequality,

$$\begin{aligned} \mathbb{E}[\|\widehat{\nabla} \widehat{f}_n(X) - \nabla f(X)\|_2^2] &\leq \mathbb{E}[\|\widehat{\nabla} \widehat{f}_n(X) - \widehat{\nabla} f(X)\|_2^2] + \mathbb{E}[\|\widehat{\nabla} f(X) - \nabla f(X)\|_2^2] \\ &\quad + 2\mathbb{E}[\|\widehat{\nabla} \widehat{f}_n(X) - \widehat{\nabla} f(X)\|_2 \|\widehat{\nabla} f(X) - \nabla f(X)\|_2] \end{aligned}$$

Now define the vector $\mathbf{I}_n(x) := (\mathbf{1}_{E_{n,i}(x)})_{i \in [d]}$. By the triangle inequality,

$$\|\widehat{\nabla} f(X) - \nabla f(X)\|_2 \leq \|\nabla f(X) \circ \bar{\mathbf{I}}_n(X)\|_2 + \|\nabla f(X) \circ \mathbf{I}_n(X) - \widehat{\nabla} f(X)\|_2,$$

and thus,

$$\begin{aligned} \mathbb{E}[\|\widehat{\nabla} f(X) - \nabla f(X)\|_2^2] &\leq \mathbb{E}[\|\nabla f(X) \circ \bar{\mathbf{I}}_n(X)\|_2^2] + \mathbb{E}[\|\nabla f(X) \circ \mathbf{I}_n(X) - \widehat{\nabla} f(X)\|_2^2] \\ &\quad + 2\mathbb{E}[\|\nabla f(X) \circ \bar{\mathbf{I}}_n(X)\|_2 \|\nabla f(X) \circ \mathbf{I}_n(X) - \widehat{\nabla} f(X)\|_2]. \end{aligned}$$

Combining the above bounds and applying Holder's inequality,

$$\begin{aligned} &\mathbb{E}[\|\widehat{\nabla} \widehat{f}_n(X) - \nabla f(X)\|_2^2] \\ &\leq \mathbb{E}[\|\widehat{\nabla} \widehat{f}_n(X) - \widehat{\nabla} f(X)\|_2^2] + \mathbb{E}[\|\nabla f(X) \circ \bar{\mathbf{I}}_n(X)\|_2^2] + \mathbb{E}[\|\nabla f(X) \circ \mathbf{I}_n(X) - \widehat{\nabla} f(X)\|_2^2] \\ &\quad + 2\mathbb{E}[\|\widehat{\nabla} \widehat{f}_n(X) - \widehat{\nabla} f(X)\|_2 \left(\|\nabla f(X) \circ \bar{\mathbf{I}}_n(X)\|_2 + \|\nabla f(X) \circ \mathbf{I}_n(X) - \widehat{\nabla} f(X)\|_2 \right)] \\ &\quad + 2\mathbb{E}[\|\nabla f(X) \circ \bar{\mathbf{I}}_n(X)\|_2 \|\nabla f(X) \circ \mathbf{I}_n(X) - \widehat{\nabla} f(X)\|_2] \\ &= \underbrace{\mathbb{E}[\|\widehat{\nabla} \widehat{f}_n(X) - \widehat{\nabla} f(X)\|_2^2]}_I + \underbrace{\mathbb{E}[\|\nabla f(X) \circ \bar{\mathbf{I}}_n(X)\|_2^2]}_{II} + \underbrace{\mathbb{E}[\|\nabla f(X) \circ \mathbf{I}_n(X) - \widehat{\nabla} f(X)\|_2^2]}_{III} \\ &\quad + 2\mathbb{E}[\|\widehat{\nabla} \widehat{f}_n(X) - \widehat{\nabla} f(X)\|_2^2]^{1/2} \mathbb{E}[\|\nabla f(X) \circ \bar{\mathbf{I}}_n(X)\|_2^2]^{1/2} \\ &\quad + 2\mathbb{E}[\|\widehat{\nabla} \widehat{f}_n(X) - \widehat{\nabla} f(X)\|_2^2]^{1/2} \mathbb{E}[\|\nabla f(X) \circ \mathbf{I}_n(X) - \widehat{\nabla} f(X)\|_2^2]^{1/2} \\ &\quad + 2\mathbb{E}[\|\nabla f(X) \circ \bar{\mathbf{I}}_n(X)\|_2^2]^{1/2} \mathbb{E}[\|\nabla f(X) \circ \mathbf{I}_n(X) - \widehat{\nabla} f(X)\|_2^2]^{1/2}. \end{aligned} \tag{14}$$

Bound on II. As in the proof of Lemma 4 in [Trivedi et al. \(2014\)](#), the assumption $\|\nabla f(x)\| \leq L$ gives

$$\mathbb{E}[\|\nabla f(X) \circ \bar{\mathbf{I}}_n(X)\|_2^2] \leq L^2 \mathbb{E}[\|\bar{\mathbf{I}}_n(X)\|_2^2].$$

For fixed $x \in \mathbb{R}^d$ and taking first just the expectation with respect to \mathcal{D}_n , Jensen's inequality gives

$$\mathbb{E}_{\mathcal{D}_n}[\|\bar{\mathbf{I}}_n(x)\|_2^2] = \sum_{j=1}^d \mathbb{E}_{\mathcal{D}_n}[\mathbf{1}_{\bar{E}_{n,j}(x)}] = \sum_{j=1}^d \mathbb{P}_{\mathcal{D}_n}(\bar{E}_{n,j}(x)).$$

Recall the notation that $\mathcal{N}_n(K) := \sum_{i=1}^n \mathbf{1}_{\{X_i \in K\}}$ is the number of training samples in a compact subset $K \subset \mathbb{R}^d$. Then, by the definition of the events $E_{n,j}(x)$,

$$\begin{aligned} \mathbb{E}_{\mathcal{D}_n}[\|\bar{\mathbf{I}}_n(x)\|_2^2] &\leq \sum_{j=1}^d (\mathbb{P}_{\mathcal{D}_n}(\mathcal{N}_n(Z_{x-te_j}) = 0) + \mathbb{P}_{\mathcal{D}_n}(\mathcal{N}_n(Z_{x+te_j}) = 0)) \\ &= \sum_{j=1}^d (\mathbb{P}_X(X \notin Z_{x-te_j})^n + \mathbb{P}_X(X \notin Z_{x+te_j})^n). \end{aligned}$$

For the probabilities in the sum, taking the expectation with respect to \mathcal{P} gives

$$\begin{aligned} \mathbb{E}_{\mathcal{P}} \left[\left(1 - \mathbb{P}_X(X \in Z_{x+se_j}^\lambda) \right)^n \right] &\leq \mathbb{E} \left[\left(n \mathbb{P}_X(X \in Z_{x+se_j}^\lambda) \right)^{-1} \right] \\ &= \frac{1}{n} \mathbb{E} \left[\sum_{C \in \mathcal{P}_\lambda} \mathbb{1}_{\{x+se_j \in C\}} \mathbb{P}_X(X \in C)^{-1} \right], \end{aligned}$$

where above $s \in \{-t, t\}$. Next, we take the expectation with respect to X and \mathcal{P} and condition on the event $B_t(X)$ to obtain:

$$\begin{aligned} \mathbb{E}[\|\bar{\mathbf{I}}_n(X)\|_2^2] &= \mathbb{E}[\|\bar{\mathbf{I}}_n(X)\|_2^2 | B_t(X)] \mathbb{P}(B_t(X)) + \mathbb{E}[\|\bar{\mathbf{I}}_n(X)\|_2^2 | \bar{B}_t(X)] \mathbb{P}(\bar{B}_t(X)) \\ &\leq \mathbb{E}[\|\bar{\mathbf{I}}_n(X)\|_2^2 | B_t(X)] + d \mathbb{P}(\bar{B}_t(X)). \end{aligned} \quad (15)$$

For the first term in the above upper bound, we have

$$\begin{aligned} \mathbb{E}[\|\bar{\mathbf{I}}_n(X)\|_2^2 | B_t(X)] &\leq \frac{1}{n} \sum_{j=1}^d \mathbb{E} \left[\sum_{C \in \mathcal{P}_\lambda} \mathbb{P}(X - te_j \in C | B_t(X)) \mathbb{P}_X(X \in C)^{-1} \right] \\ &\quad + \mathbb{E} \left[\sum_{C \in \mathcal{P}_\lambda} \mathbb{P}(X + te_j \in C | B_t(X)) \mathbb{P}_X(X \in C)^{-1} \right] \\ &\leq \frac{p_1}{np_0} \mathbb{E} \left[\sum_{C \in \mathcal{P}_\lambda} \text{vol}_d(C \cap (K - te_j \cap K)) \text{vol}_d(C \cap K)^{-1} \right] \\ &\quad + \mathbb{E} \left[\sum_{C \in \mathcal{P}_\lambda} \text{vol}_d(C \cap (K + te_j \cap K)) \text{vol}_d(C \cap K)^{-1} \right] \\ &\leq \frac{2p_1}{np_0} \mathbb{E}[N_\lambda(K)], \end{aligned}$$

where $N_\lambda(K)$ is the number of cells of the STIT tessellation with lifetime λ that intersect the compact and convex set $K \subset \mathbb{R}^d$. By Lemma 6 in [O'Reilly and Tran \(2024\)](#),

$$\mathbb{E} \left[N_\lambda([0, 1]^d) \right] \leq (1 + \lambda)^d.$$

For the second term in the upper bound (15) recall that $B_t(x)$ is the event that $x + te_j \in \text{supp}(\mu) = [0, 1]^d$ for all $j \in [d]$. Then, by the assumption on μ ,

$$\begin{aligned} \mathbb{P}(\bar{B}_t(X)) &= \mathbb{P}(\cup_{j=1}^d \{X + te_j \notin K\} \cup \{X - te_j \notin K\}) \\ &\leq p_1 \text{vol}_d(\{x \in K : x + se_j \notin K \text{ for some } s \in \{-t, t\} \text{ and } j \in \{1, \dots, d\}\}) \\ &= p_1 \left(1 - (1 - t)^d \right) = p_1 dt + O(d^2 t^2). \end{aligned}$$

Thus,

$$\mathbb{E}[\|\nabla f(X) \circ \bar{\mathbf{I}}_n(X)\|_2^2] \leq \frac{2p_1(1 + \lambda)^d}{np_0} + p_1 d^2 t + O(d^3 t^2). \quad (16)$$

Bound on III. We next prove that for fixed $x \in \mathbb{R}^d$

$$\mathbb{E}[\|\nabla f(x) \circ \mathbf{I}_n(x) - \widehat{\nabla} f(x)\|_2^2] \leq \frac{L^2 dt^2}{4}. \quad (17)$$

Indeed, by the assumption on f we have for each $i = 1, \dots, d$ and $x \in \mathbb{R}^d$,

$$\begin{aligned} f(x + te_j) - f(x - te_j) &= \int_{-t}^t \partial_j f(x + se_j) ds \\ &\leq \int_{-t}^t (\partial_j f(x) + L\|se_j\|_2) ds \\ &= 2t\partial_j f(x) + Lt^2. \end{aligned}$$

Then,

$$\left| \partial_j f(x) 1_{E_{n,j}(x)} - \frac{f(x + tu_j) - f(x - tu_j)}{2t} 1_{E_{n,j}(x)} \right| \leq \frac{Lt}{2} 1_{E_{n,j}(x)}, \quad (18)$$

and thus,

$$\begin{aligned} \mathbb{E}[\|\nabla f(x) \circ \mathbf{I}_n(x) - \widehat{\nabla} f(x)\|_2^2] &\leq \sum_{j=1}^d \mathbb{E} \left[\left| \partial_j f(x) 1_{E_{n,j}(x)} - \frac{f(x + tu_j) - f(x - tu_j)}{2t} 1_{E_{n,j}(x)} \right|^2 \right] \\ &\leq \sum_{j=1}^d \left| \partial_j f(x) - \frac{f(x + tu_j) - f(x - tu_j)}{2t} \right|^2 \mathbb{P}(E_{n,j}(x)) \\ &\leq \sum_{j=1}^d \left(\frac{Lt}{2} \right)^2 = \frac{L^2 dt^2}{4}. \end{aligned}$$

This pointwise bound also implies the bound in expectation:

$$\mathbb{E}[\|\nabla f(X) \circ \mathbf{I}_n(X) - \widehat{\nabla} f(X)\|_2^2] \leq \frac{L^2 dt^2}{4}.$$

Bound on I. Lastly we obtain a bound on $\mathbb{E}[\|\widehat{\nabla} \widehat{f}_n(X) - \widehat{\nabla} f(X)\|_2^2]$. First, for fixed $x \in \mathbb{R}^d$ we have

$$\begin{aligned} &\left| \frac{f(x + te_j) - f(x - te_j) - \widehat{f}_n(x + te_j) + \widehat{f}_n(x - te_j)}{2t} \right| 1_{E_{n,i}(x)} \\ &\leq \frac{|f(x + te_j) - \widehat{f}_n(x + te_j)| 1_{E_{n,i}(x)}}{2t} + \frac{|f(x - te_j) - \widehat{f}_n(x - te_j)| 1_{E_{n,i}(x)}}{2t}. \end{aligned} \quad (19)$$

Then,

$$\begin{aligned} \|\widehat{\nabla} \widehat{f}_n(x) - \widehat{\nabla} f(x)\|_2^2 &\leq \frac{1}{4t^2} \sum_{j=1}^d |f(x + te_j) - \widehat{f}_n(x + te_j)|^2 1_{E_{n,i}(x)} \\ &\quad + \frac{1}{4t^2} \sum_{j=1}^d |f(x - te_j) - \widehat{f}_n(x - te_j)|^2 1_{E_{n,i}(x)}. \end{aligned}$$

Taking the expectation with respect to \mathcal{P} and \mathcal{D}_n gives the upper bound

$$\mathbb{E}[\|\widehat{\nabla} f_n(x) - \widehat{\nabla} f(x)\|_2^2] \leq \frac{1}{4t^2} \sum_{j=1}^d \left(\mathbb{E}[|f(x + te_j) - \widehat{f}_n(x + te_j)|^2] + \mathbb{E}[|f(x - te_j) - \widehat{f}_n(x - te_j)|^2] \right).$$

Taking the expectation with respect to X gives

$$\mathbb{E}[\|\widehat{\nabla} f_n(X) - \widehat{\nabla} f(X)\|_2^2] \leq \frac{1}{4t^2} \sum_{j=1}^d \left(\mathbb{E}[|f(X + te_j) - \widehat{f}_n(X + te_j)|^2] + \mathbb{E}[|f(X - te_j) - \widehat{f}_n(X - te_j)|^2] \right).$$

By Proposition 12, for $s \in \{-t, t\}$ and $t = o(1)$ as $n \rightarrow \infty$,

$$\mathbb{E}[|f(X + se_j) - \widehat{f}_n(X + te_j)|^2] \lesssim \frac{\lambda^d}{n} + \frac{L^2}{\lambda^3} + \frac{L^2}{\lambda^2 M},$$

and thus,

$$\mathbb{E}[\|\widehat{\nabla} f_n(X) - \widehat{\nabla} f(X)\|_2^2] \lesssim \frac{d}{t^2} \left(\frac{\lambda^d}{n} + \frac{L^2}{\lambda^3} + \frac{L^2}{\lambda^2 M} \right). \quad (20)$$

Final bound

Combining the bounds (16), (17), and (20) with (14) gives:

$$\mathbb{E}[\|\widehat{\nabla} f_n(X) - \nabla f(X)\|_2^2] \lesssim \frac{d}{t^2} \left(\frac{\lambda^d}{n} + \frac{L^2}{\lambda^3} + \frac{L^2}{\lambda^2 M} \right) + \frac{\lambda^d}{n} + L^2 dt^2.$$

Minimizing the above bound with respect to λ and t gives the final asymptotic result. \square

A.3. Proof of Theorem 4 and Corollary 5

Proof of Theorem 4. We first observe the following bound: by the triangle inequality

$$\|\widehat{H}_n - H\| \leq \|\widehat{H}_n - H_n\| + \|H_n - H\|, \quad (21)$$

where

$$H_n := \frac{1}{n} \sum_{i=1}^n \nabla f(x_i) \nabla f(x_i)^T.$$

By Lemma 2 in Trivedi et al. (2014), which follows directly from a concentration bound for random matrices (see Tropp (2012)) we have: with probability at least $1 - \delta$ over the i.i.d samples $\{X_i\}_{i=1}^n$,

$$\|H_n - H\| \leq \frac{6L^2}{\sqrt{n}} \left(\sqrt{\ln d} + \sqrt{\ln \frac{1}{\delta}} \right).$$

Then, letting $t = \frac{6L^2}{\sqrt{n}} \left(\sqrt{\ln d} + \sqrt{\ln \frac{1}{\delta}} \right)$ gives

$$\begin{aligned} \mathbb{E}[\|H_n - H\|] &= \int_0^\infty \mathbb{P}(\|H_n - H\| \geq t) dt \leq \int_0^\infty e^{-\left(\frac{\sqrt{ny}}{6L^2} - \sqrt{\ln d}\right)^2} dy \\ &\leq \int_{\mathbb{R}} e^{-\frac{n}{36L^4} \left(y - 6L^2 \sqrt{\frac{\ln d}{n}}\right)^2} dy = \frac{6\sqrt{\pi}L^2}{\sqrt{n}}. \end{aligned}$$

For the first term in (21), the same argument as in Lemma 3 of Trivedi et al. (2014) gives

$$\begin{aligned}
\|\widehat{H}_n - H_n\| &= \left\| \frac{1}{n} \sum_{i=1}^n \widehat{\nabla} \widehat{f}_n(x_i) \widehat{\nabla} \widehat{f}_n(x_i)^T - \frac{1}{n} \sum_{i=1}^n \nabla f(x_i) \nabla f(x_i)^T \right\| \\
&\leq \frac{1}{n} \sum_{i=1}^n \left\| \widehat{\nabla} \widehat{f}_n(x_i) \widehat{\nabla} \widehat{f}_n(x_i)^T - \nabla f(x_i) \nabla f(x_i)^T \right\| \\
&\leq \frac{1}{n} \sum_{i=1}^n \left\| \widehat{\nabla} \widehat{f}_n(x_i) + \nabla f(x_i) \right\|_2 \left\| \widehat{\nabla} \widehat{f}_n(x_i) - \nabla f(x_i) \right\|_2 \\
&\leq \frac{1}{n} \sum_{i=1}^n 2 \|\nabla f(x_i)\|_2 \|\widehat{\nabla} \widehat{f}_n(x_i) - \nabla f(x_i)\|_2 + \frac{1}{n} \sum_{i=1}^n \|\widehat{\nabla} \widehat{f}_n(x_i) - \nabla f(x_i)\|_2 \|\widehat{\nabla} \widehat{f}_n(x_i) - \nabla f(x_i)\|_2 \\
&\leq \frac{2L}{n} \sum_{i=1}^n \|\widehat{\nabla} \widehat{f}_n(x_i) - \nabla f(x_i)\|_2 + \frac{1}{n} \sum_{i=1}^n \|\widehat{\nabla} \widehat{f}_n(x_i) - \nabla f(x_i)\|_2^2,
\end{aligned}$$

where we used in the second inequality that for $a, b \in \mathbb{R}^d$,

$$\|aa^T - bb^T\| \leq \|(b+a)(a-b)^T\| = \|b+a\| \|a-b\|,$$

and for the last inequality, we used the smoothness assumption on f .

Taking the expectation with respect to \mathcal{X}_n gives

$$\mathbb{E}_{\mathcal{X}_n}[\|\widehat{H}_n - H_n\|] \leq 2L \mathbb{E}_X[\|\widehat{\nabla} \widehat{f}_n(X) - \nabla f(X)\|_2] + \mathbb{E}_X[\|\widehat{\nabla} \widehat{f}_n(X) - \nabla f(X)\|_2^2].$$

Taking the expectation with respect to \mathcal{D}_n and \mathcal{P} and using Proposition 13 and Jensen's inequality gives: for $\lambda \sim n^{\frac{1}{d+3}}$, $M \gtrsim n^{\frac{1}{d+3}}$ and $t \sim n^{-\frac{3}{4d+12}}$,

$$\begin{aligned}
\mathbb{E}[\|\widehat{H}_n - H_n\|] &\leq 2L \mathbb{E}[\|\widehat{\nabla} \widehat{f}_n(X) - \nabla f(X)\|_2] + \mathbb{E}[\|\widehat{\nabla} \widehat{f}_n(X) - \nabla f(X)\|_2^2] \\
&\leq 2L \mathbb{E}[\|\widehat{\nabla} \widehat{f}_n(X) - \nabla f(X)\|_2^2]^{1/2} + \mathbb{E}[\|\widehat{\nabla} \widehat{f}_n(X) - \nabla f(X)\|_2^2] \\
&\lesssim n^{-\frac{3}{4d+12}}.
\end{aligned}$$

Thus,

$$\mathbb{E}[\|\widehat{H}_n - H\|] \leq \mathbb{E}[\|\widehat{H}_n - H_n\|] + \mathbb{E}[\|H_n - H\|] \lesssim n^{-\frac{3}{4d+12}}.$$

□

Proof of Corollary 5. By the triangle inequality and reverse triangle inequality for the $\|\cdot\|_{2,1}$ norm,

$$\begin{aligned}
\|\widehat{A}_n - A\|_{2,1} &= d \left\| \frac{\widehat{H}_n}{\|\widehat{H}_n\|_{2,1}} - \frac{H}{\|H\|_{2,1}} \right\|_{2,1} = d \left\| \frac{\|H\|_{2,1} \widehat{H}_n - \|\widehat{H}_n\|_{2,1} H}{\|\widehat{H}_n\|_{2,1} \|H\|_{2,1}} \right\|_{2,1} \\
&\leq d \left\| \frac{\|H\|_{2,1} \widehat{H}_n - \|\widehat{H}_n\|_{2,1} \widehat{H}_n + \|\widehat{H}_n\|_{2,1} \widehat{H}_n - \|\widehat{H}_n\|_{2,1} H}{\|\widehat{H}_n\|_{2,1} \|H\|_{2,1}} \right\|_{2,1} \\
&\leq d \left\| \frac{\|H\|_{2,1} \widehat{H}_n - \|\widehat{H}_n\|_{2,1} \widehat{H}_n}{\|\widehat{H}_n\|_{2,1} \|H\|_{2,1}} \right\|_{2,1} + d \left\| \frac{\|\widehat{H}_n\|_{2,1} \widehat{H}_n - \|\widehat{H}_n\|_{2,1} H}{\|\widehat{H}_n\|_{2,1} \|H\|_{2,1}} \right\|_{2,1} \\
&= \frac{d \|\|H\|_{2,1} - \|\widehat{H}_n\|_{2,1}\|}{\|H\|_{2,1}} + \frac{d \|\widehat{H}_n - H\|_{2,1}}{\|H\|_{2,1}} \leq \frac{2d \|\widehat{H}_n - H\|_{2,1}}{\|H\|_{2,1}}.
\end{aligned}$$

The result then follows from Theorem 4 and equivalence of the column sum norm and operator norm on the matrix space $\mathbb{R}^{d \times d}$. □

Appendix B: Proof of Theorem 7

To directly apply results of O'Reilly (2024), we recall an equivalent assumption to (2) is

$$f(x) = \tilde{g}(P_S x), \quad (22)$$

where $P_S \in \mathbb{R}^{d \times d}$ is the orthogonal projection matrix onto the subspace S and $\tilde{g}: S \rightarrow \mathbb{R}$ denotes a function (different than g) that will satisfy assumption 3 for some constant $\tilde{L} > 0$.

Proof. By Lemma 6 and Theorem 7 in O'Reilly (2024), we have the upper bound

$$\mathbb{E}[(\hat{f}_n(X) - f(X))^2] \leq \frac{9\tilde{L}^2 d^4}{\lambda^2 \sigma_s (P_S A_n)^2} + \frac{(5\|f\|_\infty^2 + 2\sigma^2)d^s}{n} \left(\sum_{k=s}^d c_{d,k} \lambda^k \|P_{S^\perp} A_n\|_{2,1}^{k-s} + O(\lambda^{s-1}) \right),$$

where $c_{d,k} := \frac{\kappa_k \pi^{k/2}}{k! d^{k/2}}$, and the expectation is taken with respect to X , \mathcal{D}'_n and \mathcal{P}' . By Corollary 4 and Markov's inequality,

$$\mathbb{P}(\|A_n - A\|_{2,1} > n^{-\frac{3(1-\delta)}{4d+12}}) \leq n^{\frac{3(1-\delta)}{4d+12}} \mathbb{E}[\|A_n - A\|_{2,1}] \lesssim n^{-\frac{3\delta}{4d+12}}$$

Then, for all n large enough, there exist constants $C, c > 0$ such that with probability at least $1 - Cn^{-\frac{3\delta}{4d+12}}$ with respect to \mathcal{D}_n , \mathcal{P} , and \mathcal{X}_n , we have that $\sigma_s(P_S A_n) \geq c > 0$, and

$$\|P_S^\perp A_n\|_{2,1} = \|P_S^\perp (A_n - A)\|_{2,1} \leq \|A_n - A\|_{2,1} \leq n^{-\frac{3(1-\delta)}{4d+12}}.$$

Corollary 8 in O'Reilly (2024) then implies that with probability at least $1 - Cn^{-\frac{3\delta}{4d+12}}$ with respect to \mathcal{D}_n , \mathcal{P} , and \mathcal{X}_n , for $\lambda_n \sim n^{\frac{1}{d+2} + \frac{3(1-\delta)(d-s)}{4(d+3)(d+2)}}$ and $M_n \gtrsim \lambda_n$,

$$\mathbb{E}[(\hat{f}_n(X) - f(X))^2] \lesssim n^{-\frac{2}{d+2} - \frac{3(1-\delta)(d-s)}{2(d+3)(d+2)}}.$$

□

Appendix C: Proofs of Theorem 9 and Theorem 10

Proof of Theorem 9. Similarly to the argument of Corollary 5, we first see that

$$\begin{aligned} \max_{i \in \{1, \dots, d\}} \left| \frac{\omega_i}{\sum_{j=1}^d \omega_j} - \frac{\mathbb{E}[|(\nabla f(X))_i|^2]}{\mathbb{E}[\|\nabla f(X)\|_2^2]} \right| &\leq \sum_{i=1}^d \left| \frac{\omega_i}{\sum_{j=1}^d \omega_j} - \frac{\mathbb{E}[|(\nabla f(X))_i|^2]}{\mathbb{E}[\|\nabla f(X)\|_2^2]} \right| \\ &\leq \frac{2 \sum_{i=1}^d |\omega_i - \mathbb{E}[|(\nabla f(X))_i|^2]|}{\mathbb{E}[\|\nabla f(X)\|_2^2]}. \end{aligned}$$

Now noting that $\sum_{i=1}^d \omega_i = \frac{1}{n} \sum_{j=1}^n \|\widehat{\nabla} \widehat{f}_n(x_j)\|^2$, we have

$$\begin{aligned}
& \sum_{i=1}^d \left| \omega_i - \mathbb{E}[|(\nabla f(X))_i|^2] \right| \\
&= \sum_{i=1}^d \left| \frac{1}{n} \sum_{j=1}^n |(\widehat{\nabla} \widehat{f}_n(x_j))_i|^2 - \mathbb{E}[|(\nabla f(X))_i|^2] \right| \\
&\leq \frac{1}{n} \sum_{j=1}^n \sum_{i=1}^d \left| \left(|(\widehat{\nabla} \widehat{f}_n(x_j))_i - (\nabla f(x_j))_i| + |(\nabla f(x_j))_i| \right)^2 - \mathbb{E}[|(\nabla f(X))_i|^2] \right| \\
&= \frac{1}{n} \sum_{j=1}^n \sum_{i=1}^d \left| |(\widehat{\nabla} \widehat{f}_n(x_j))_i - (\nabla f(x_j))_i|^2 + 2|(\widehat{\nabla} \widehat{f}_n(x_j))_i - (\nabla f(x_j))_i| |(\nabla f(x_j))_i| \right. \\
&\quad \left. + |(\nabla f(x_j))_i|^2 - \mathbb{E}[|(\nabla f(X))_i|^2] \right| \\
&\leq \frac{1}{n} \sum_{j=1}^n \|\widehat{\nabla} \widehat{f}_n(x_j) - \nabla f(x_j)\|_2^2 + \frac{2}{n} \sum_{j=1}^n \|\widehat{\nabla} \widehat{f}_n(x_j) - \nabla f(x_j)\|_2 \|\nabla f(x_j)\|_2 \\
&\quad + \frac{1}{n} \sum_{j=1}^n \sum_{i=1}^d \left| |(\nabla f(x_j))_i|^2 - \mathbb{E}[|(\nabla f(X))_i|^2] \right|.
\end{aligned}$$

Taking the expectation with respect to \mathcal{X}_n , \mathcal{P} , and \mathcal{D}_n and applying Proposition 13 gives

$$\mathbb{E} \left[\max_{i \in \{1, \dots, d\}} \left| \frac{\omega_i}{\sum_{j=1}^d \omega_j} - \frac{\mathbb{E}[|(\nabla f(X))_i|^2]}{\mathbb{E}[\|\nabla f(X)\|_2^2]} \right| \right] \lesssim n^{-\frac{3}{4d+12}}.$$

□

Proof of Theorem 10. By Theorem 9 and Markov's inequality,

$$\begin{aligned}
& \mathbb{P} \left(\max_{i \in \{1, \dots, d\}} \left| \frac{\omega_i}{\sum_{j=1}^d \omega_j} - \frac{\mathbb{E}[|(\nabla f(X))_i|^2]}{\mathbb{E}[\|\nabla f(X)\|_2^2]} \right| > n^{-\frac{3(1-\delta)}{4d+12}} \right) \\
&\leq n^{\frac{3(1-\delta)}{4d+12}} \mathbb{E} \left[\max_{i \in \{1, \dots, d\}} \left| \frac{\omega_i}{\sum_{j=1}^d \omega_j} - \frac{\mathbb{E}[|(\nabla f(X))_i|^2]}{\mathbb{E}[\|\nabla f(X)\|_2^2]} \right| \right] \lesssim n^{-\frac{3\delta}{4d+12}}.
\end{aligned}$$

Then, for all n large enough, there exists constants $C, c > 0$ such that with probability at least $1 - Cn^{-\frac{3\delta}{4d+12}}$ with respect to \mathcal{D}_n , \mathcal{P} , and \mathcal{X}_n , we have that $\min_{i \in S} \frac{\omega_i}{\sum_{j=1}^d \omega_j} \geq c > 0$, and

$$\max_{i \notin S} \frac{\omega_i}{\sum_{j=1}^d \omega_j} \leq n^{-\frac{3(1-\delta)}{4d+12}}.$$

Finally, by Corollary 14 in O'Reilly (2024), letting $M_n \gtrsim \lambda_n$ and $\lambda_n \sim n^{\frac{1}{d+3} + \frac{3(d-s)}{4(d+3)^2}}$ gives that with probability at least $1 - Cn^{-\frac{3\delta}{4d+12}}$ with respect to \mathcal{D}_n , \mathcal{P} , and \mathcal{X}_n ,

$$\mathbb{E}[(\widehat{f}_n(X) - f(X))^2] \lesssim n^{-\frac{3}{d+3} - \frac{9(d-s)}{4(d+3)^2}}.$$

□

Appendix D: Maximum Principal Angle

In this section, we describe the distance between two subspaces that is computed as part of our numerical experiments to assess the recovery of the relevant feature subspaces. For two subspaces $[U, W]$ of dimension k , we compute the QR decomposition of both. That is,

$$\begin{aligned} U &= Q_u R_u \\ W &= Q_w R_w, \end{aligned}$$

where Q_u and $Q_w \in \mathbb{R}^{n \times k}$ are orthonormal bases such that $Q_u^T Q_u = Q_w^T Q_w = I_k$ that span the same subspace as the original columns of U and W , and R_u and $R_w \in \mathbb{R}^{k \times k}$ are lower triangular matrices. Next, we compute the following matrix that contains the inner products between the two collections of basis vectors

$$D = \langle Q_u, Q_w \rangle = Q_u^T Q_w \in \mathbb{R}^{k \times k},$$

and then apply the singular value decomposition

$$D = U \Sigma V^T.$$

By interpreting D as the cross-covariance matrix, its singular vectors represent the main orthogonal axes of cross-covariation between the two subspaces, while the singular values represent angles. In order to compute the principal angles of the subspaces, we define

$$\theta := \cos^{-1}(\Sigma) = \cos^{-1}([\sigma_1 \ \sigma_2 \ \dots \ \sigma_k])$$

The metric we use to compare subspaces is the maximum principal angle, which is simply the maximum value of θ . For more details on this distance, we refer the reader to [Ye and Lim \(2016\)](#).

Appendix E: Additional Details on the Numerical Experiments

E.1. Simulation Study

Figure 6 shows the maximum principal angles between the subspaces spanned by the true expected outer product matrix H and the estimated expected outer product matrix $\hat{H}_{n,t}$ after $K = 1$ iteration of the proposed TrIM method. Figure 7 compares the test mean squared error (MSE) of the proposed method and the oracle method that has knowledge of the true H after one round of iteration for the four scenarios described in Section 5.

E.2. SEIR Model for the Spread of Ebola in Western Africa

The model we employ is a modified SEIR model for the spread of Ebola in Western Africa. The model incorporates specific assumptions to focus on key dynamics relevant to the spread of disease, following [Diaz et al. \(2018\)](#); [Constantine and Howard \(2016\)](#). In particular, the model makes the following three assumptions. First, stochastic effects, births and non-ebola deaths are negligible. Second, individuals who are removed (or deceased) can fall into one of three states: those who are infectious but have been improperly buried, posing a risk of further transmission; those who are non-infectious due to proper burial, effectively halting transmission from these individuals; and those who have recovered from the disease and are assumed to have immunity, thus not becoming susceptible again. Third, hospitalized individuals can still spread the disease. However, deaths in

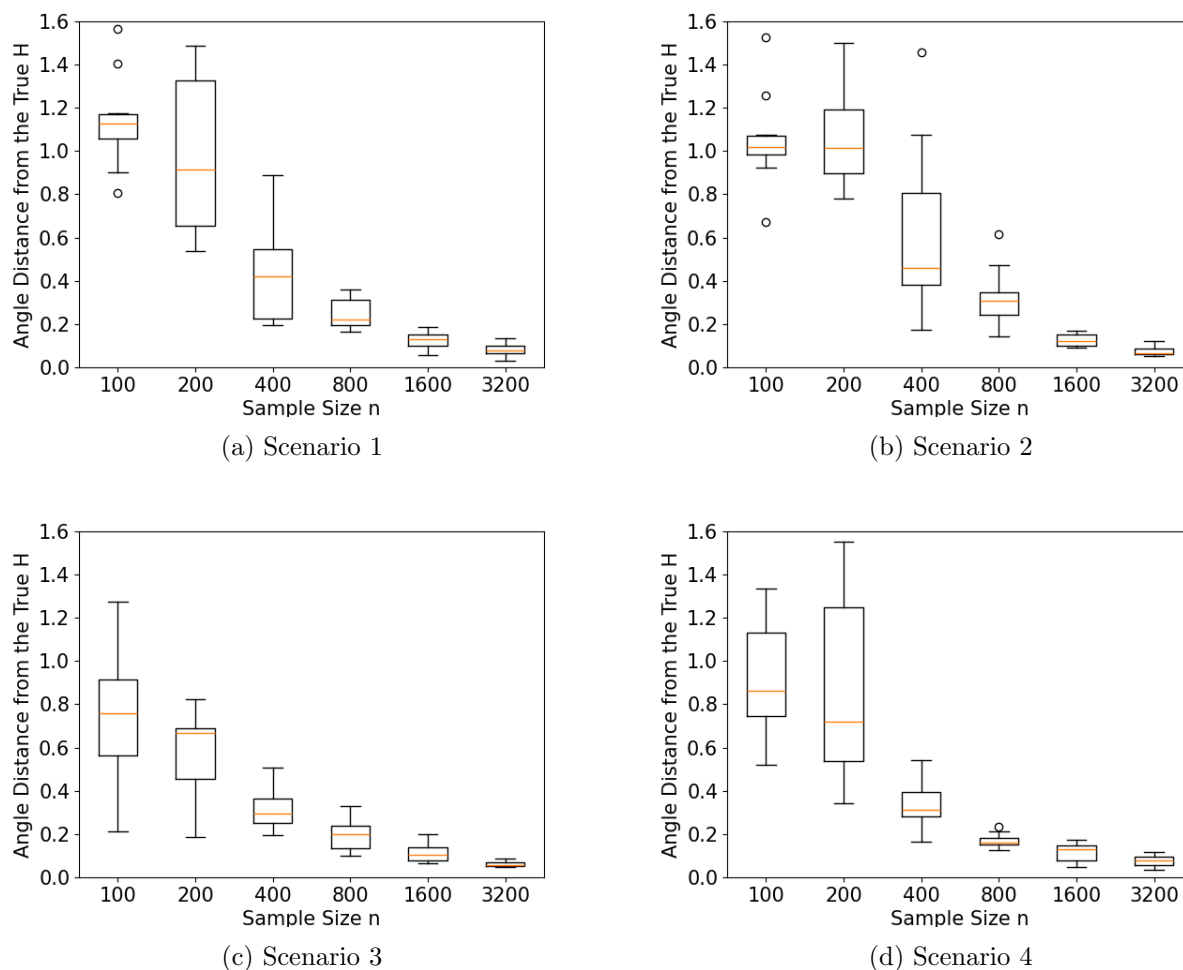


Fig 6: Simulation study: Maximum principal angles between the subspaces spanned by the expected outer product matrix H and estimated expected outer product matrix $\hat{H}_{n,t}$ after one round of iteration of the proposed method.

hospitals are properly buried and hospitalization increases the chances of recovery. Under these

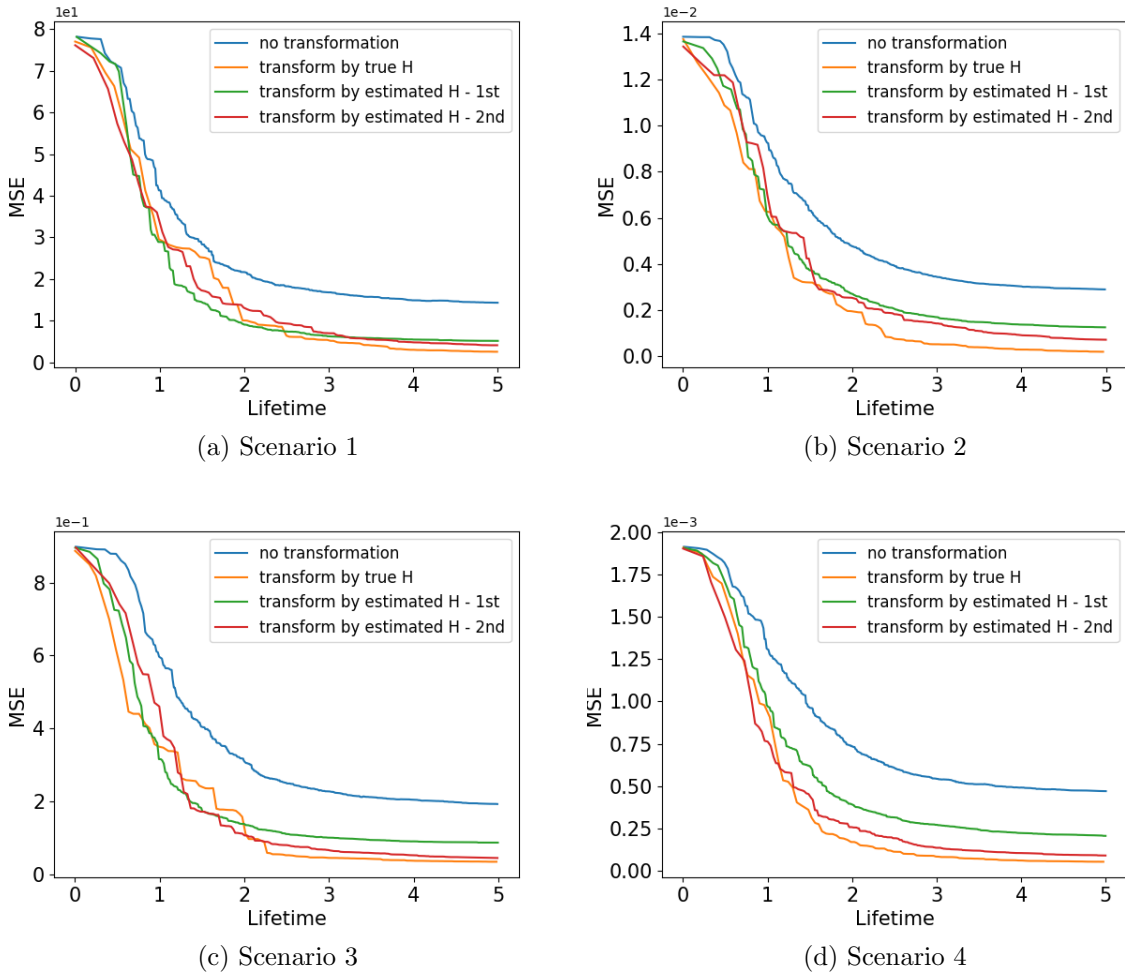


Fig 7: Simulation study: Comparison of the test mean squared error (MSE) of the proposed method and the oracle method after one round of iteration of the proposed method.

assumptions, the ordinary differential equations governing our model are

$$\begin{aligned}
 \frac{dS}{dt} &= -\beta_1 SI - \beta_2 SR_I - \beta_3 SH, \\
 \frac{dE}{dt} &= \beta_1 SI + \beta_2 SR_I + \beta_3 SH - \delta E, \\
 \frac{dI}{dt} &= \delta E - \gamma_1 I - \psi I, \\
 \frac{dH}{dt} &= \psi I - \gamma_2 H, \\
 \frac{dR_I}{dt} &= \rho_1 \gamma_1 I - \omega R_I, \\
 \frac{dR_B}{dt} &= \omega R_I + \rho_2 \gamma_2 H, \\
 \frac{dR_R}{dt} &= (1 - \rho_1) \gamma_1 I + (1 - \rho_2) \gamma_2 H,
 \end{aligned}$$

where S is the susceptible fraction of the population, E is the exposed population (infected but asymptomatic), I is the infected fraction, H is the hospitalized fraction, R_I is the infectious dead (not properly buried), R_B is the non-infectious dead (properly buried), and R_R is the recovered fraction. The basic reproduction number (a metric measuring how many new cases of disease each current case causes) is given by

$$R_0(p) = \frac{\beta_1 + \frac{\beta_2 \rho_1 \gamma_1}{\omega} + \frac{\beta_3 \psi}{\gamma_2}}{\gamma_1 + \psi}.$$

We use uniform distributions, $\mu = U(\min, \max)$, for the input parameters to the model whose parameters are given in the following table.

Parameter	Liberia	Sierra Leone
β_1	$U(.1, .4)$	$U(.1, .4)$
β_2	$U(.1, .4)$	$U(.1, .4)$
β_3	$U(.05, .2)$	$U(.05, .2)$
ρ_1	$U(.41, 1)$	$U(.41, 1)$
γ_1	$U(.0276, .1702)$	$U(.0275, .1569)$
γ_2	$U(.081, .21)$	$U(.1236, .384)$
ω	$U(.25, .5)$	$U(.25, .5)$
ψ	$U(.0833, .7)$	$U(.0833, .7)$

The expected outer product matrix H for this problem has the form

$$H = \int \nabla R_0(x) \nabla R_0(x)^T \mu(x) dx,$$

where ∇R_0 is the gradient of R_0 with respect to the normalized parameters, and μ is the probability density function on the parameters. We approximate H using Gauss-Legendre quadrature with 8 points in each of the 8 dimensions of the parameter space. Gradients with respect to normalized parameters are computed according to the chain rule: if p is an un-normalized parameter and x is its normalized version, then $\frac{\partial R_0}{\partial x} = \frac{\partial R_0}{\partial p} \frac{\partial p}{\partial x}$, and $p = l + \frac{u-l}{2}(x+1) \Rightarrow \frac{\partial p}{\partial x} = \frac{u-l}{2}$, where u and l are the upper and lower bounds on the parameter. The resulting expected outer product matrix corresponds to the one identified using the active subspace procedures described in Constantine et al. (2014).

Figures 8 and Figure 9 show that our proposed method performs well with this model. The maximum principal angles between the subspaces spanned by the true expected outer product matrix H and estimated expected outer product matrix $\hat{H}_{n,t}$ decrease as the training sample size n increases. The test MSE of the proposed method is consistently lower than the baseline method. Moreover, the test MSE after a second iteration of the proposed TrIM method is closer to the test MSE of the oracle method than the test MSE of the proposed method with a single iteration, when the lifetime is long enough. Interestingly, when the lifetime is short, the test MSE with a single iteration of the proposed method is lower than the test MSE with two iterations of TrIM as well as the oracle method.

E.3. Real Data Experiments

Figure 10 shows the comparison of the test mean squared error (MSE) of the proposed method and the oracle method for the real datasets. The proposed method performs well in this setting, as shown in Figure 5 and Figure 10. The test MSE of TrIM is consistently lower than the baseline Mondrian forest.

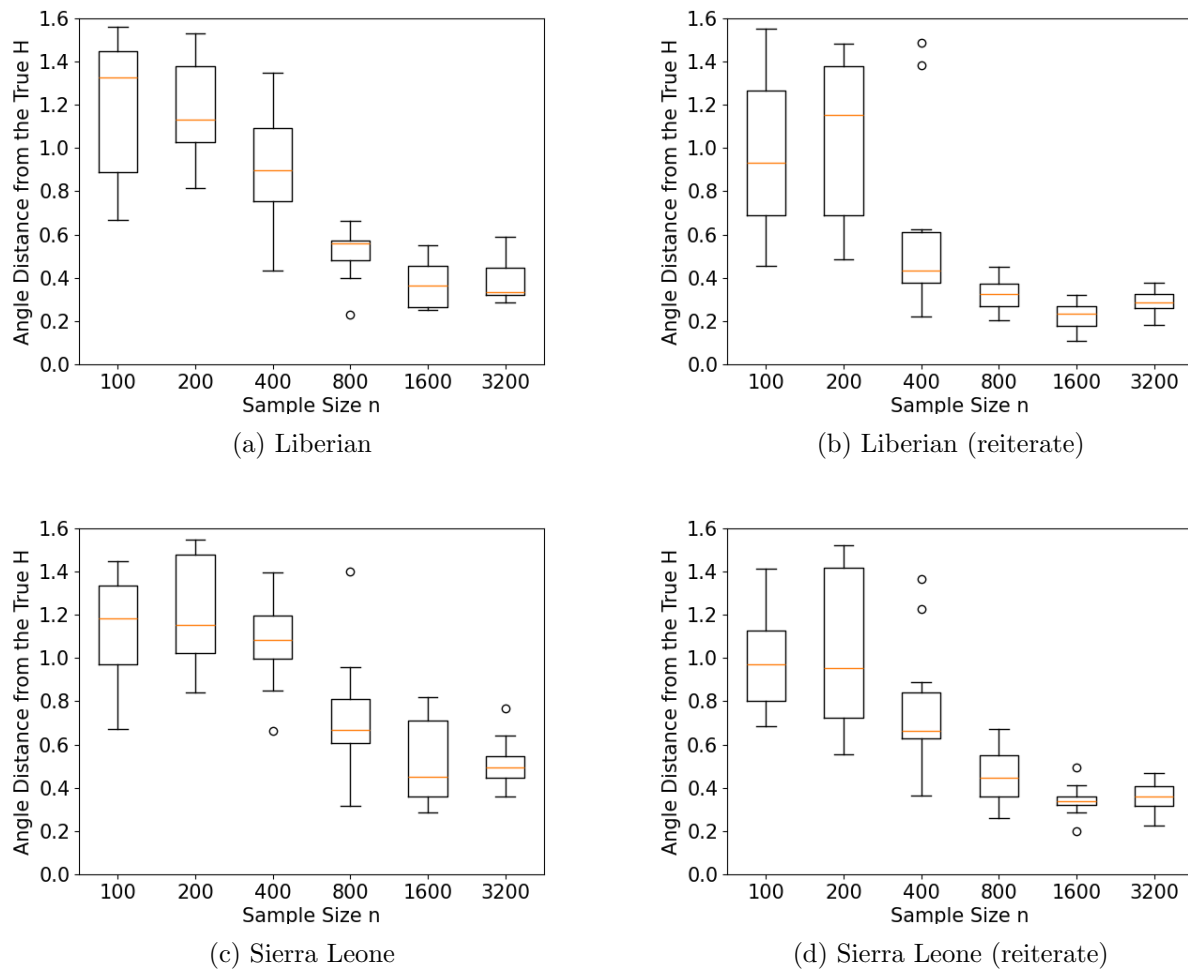


Fig 8: SEIR model for the spread of Ebola in Western Africa: Maximum principal angles between the subspaces spanned by the expected outer product matrix H and estimated expected outer product matrix $\hat{H}_{n,t}$.

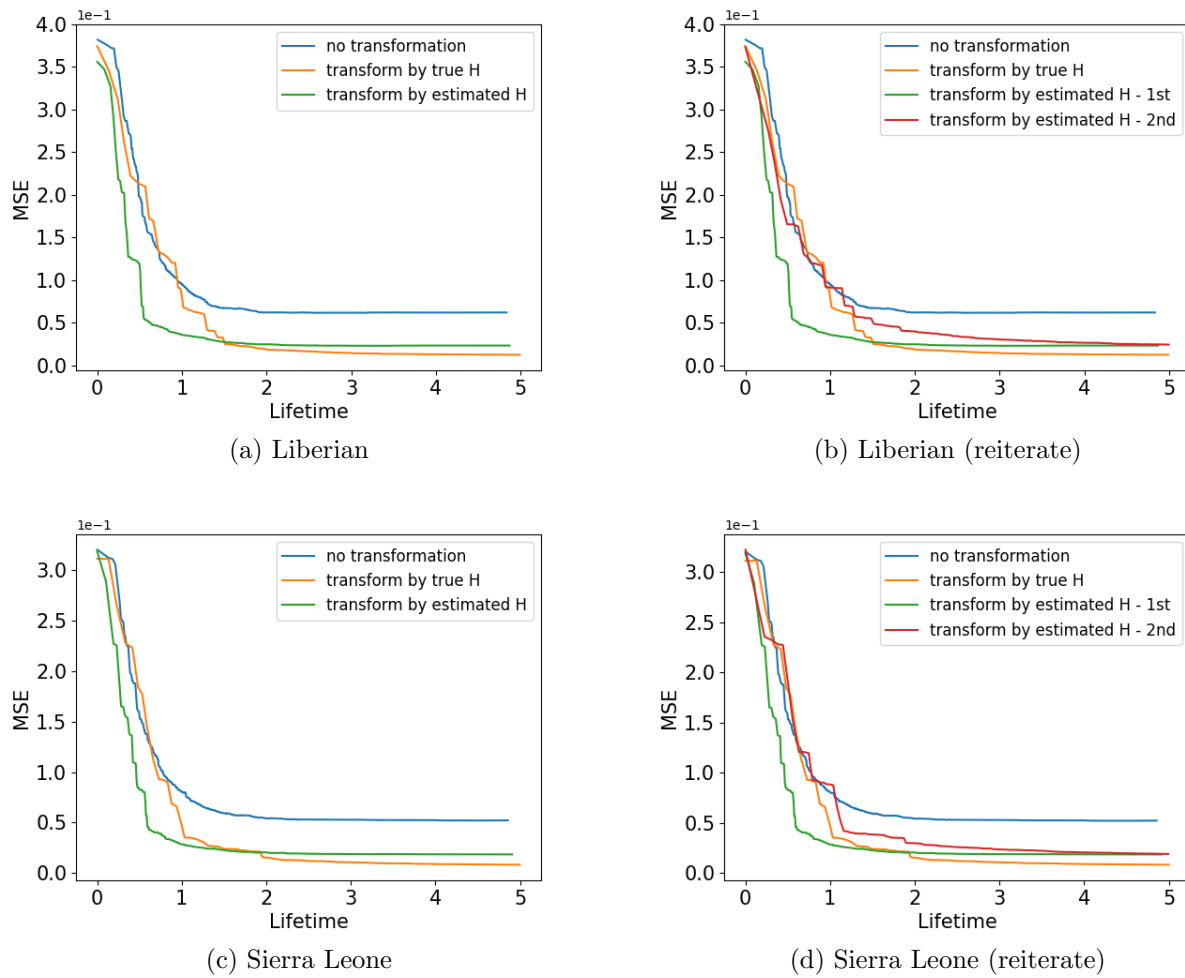
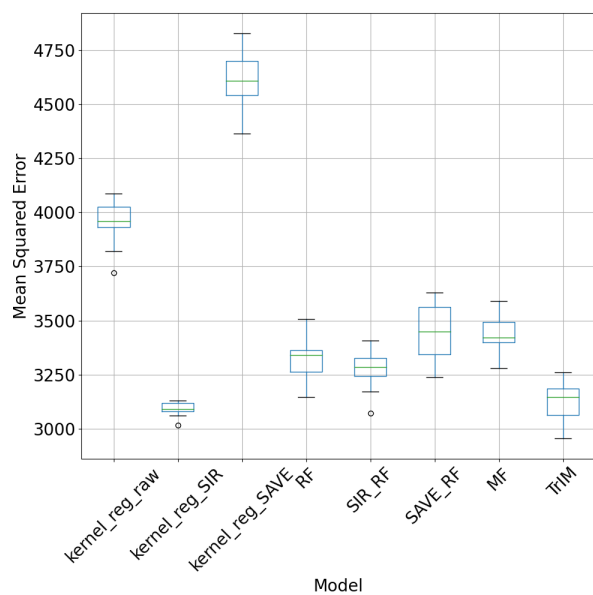
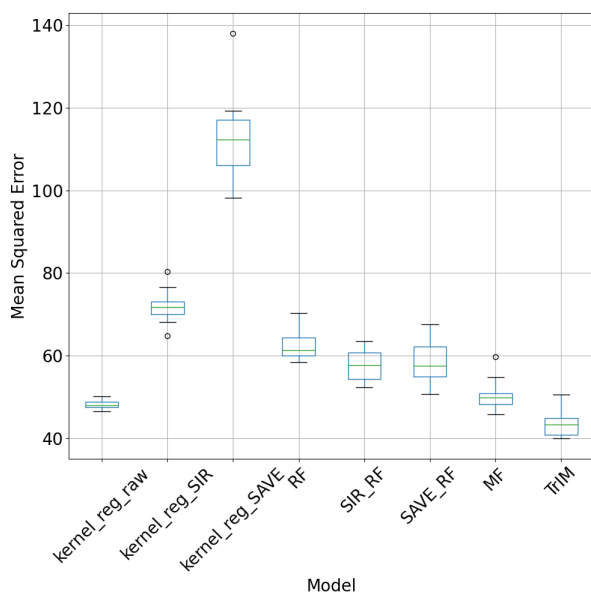


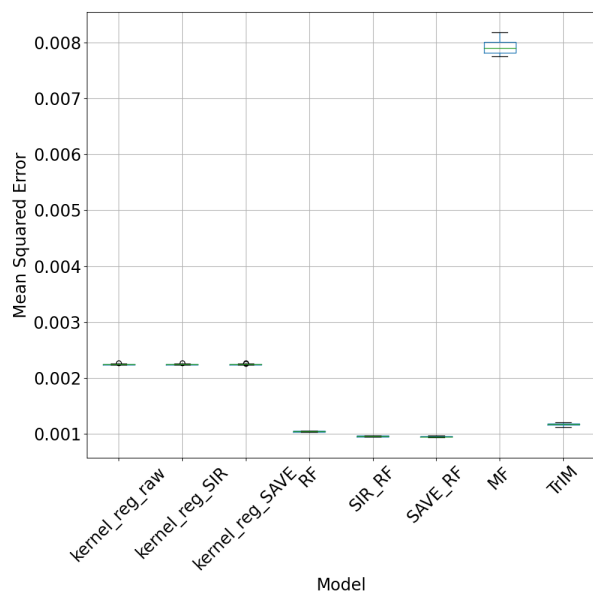
Fig 9: SEIR model for the spread of Ebola in Western Africa: Comparison of the test mean squared error (MSE) of the proposed method and the oracle method.



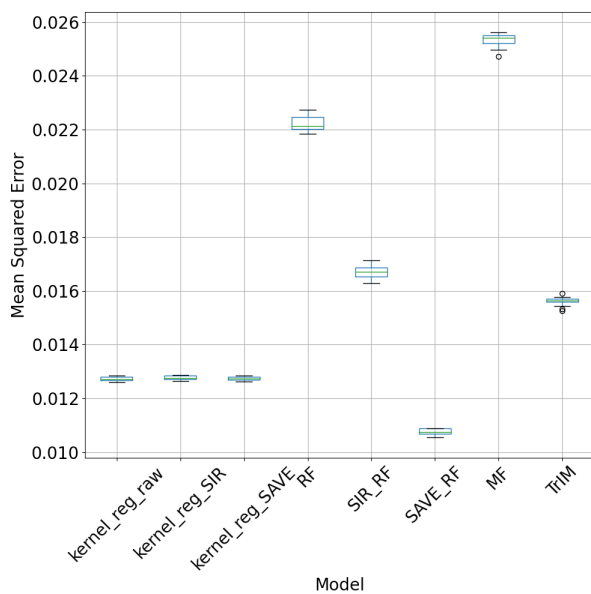
(a) Diabetes



(b) Mu284



(c) Bank8FM



(d) Kin8nm

Fig 10: Comparison of the test mean squared error (MSE) of different methods for real data applications, where the box plot displays the variation across 15 trials. Results for two additional datasets are presented in Figure 5.